

A data compendium of *Mycobacterium tuberculosis* antibiotic resistance

The CRyPTIC Consortium

5 **Abstract**

6 The Comprehensive Resistance Prediction for Tuberculosis: an International
7 Consortium (CRyPTIC) presents here a compendium of 15,211 *Mycobacterium*
8 *tuberculosis* global clinical isolates, all of which have undergone whole genome
9 sequencing (WGS) and have had their minimum inhibitory concentrations to 13
10 antitubercular drugs measured in a single assay. It is the largest matched phenotypic
11 and genotypic dataset for *M. tuberculosis* to date. Here, we provide a summary
12 detailing the breadth of data collected, along with a description of how the isolates
13 were collected and uniformly processed in CRyPTIC partner laboratories across 23
14 countries. The compendium contains 6,814 isolates resistant to at least one drug,
15 including 2,129 samples that fully satisfy the clinical definitions of rifampicin resistant
16 (RR), multi-drug resistant (MDR), pre-extensively drug resistant (pre-XDR) or
17 extensively drug resistant (XDR). Accurate prediction of resistance status
18 (sensitive/resistant) to eight antitubercular drugs by using a genetic mutation
19 catalogue is presented along with the presence of suspected resistance-conferring
20 mutations for isolates resistant to the newly introduced drugs bedaquiline, clofazimine,
21 delamanid and linezolid. Finally, a case study of rifampicin mono-resistance
22 demonstrates how this compendium could be used to advance our genetic
23 understanding of rare resistance phenotypes. The compendium is fully open-source
24 and it is hoped that the dataset will facilitate and inspire future research for years to
25 come.

26

27

28

29

30 **Introduction**

31 Tuberculosis (TB) is a curable and preventable disease; 85% of those afflicted
32 can be successfully treated with a six-month regimen. Despite this, TB is the world's
33 top infectious disease killer (current SARS-CoV-2 pandemic excepted) with 10 million
34 new cases and 1.2 million deaths estimated in 2019 alone (1). Furthermore, drug
35 resistant TB (DR-TB) is a continual threat; almost half a million cases resistant to the
36 first-line drug rifampicin (RR-TB) were estimated, with three quarters of these
37 estimated to be multidrug-resistant (MDR-TB, resistant to first-line drugs isoniazid and
38 rifampicin) (1). Worryingly, only 44% of DR-TB cases were officially notified and just
39 over half of these cases were successfully treated (57%) (1).

40

41 To address these issues, the World Health Organisation (WHO) is encouraging
42 the development of better, faster and more targeted diagnostic and treatment
43 strategies through its EndTB campaign (1). Of particular interest is universal drug
44 susceptibility testing (DST). Conventionally, DST relies on lengthy (4 weeks minimum)
45 culture-based methods that require strict biosafety conditions for *Mycobacterium*
46 *tuberculosis*. The development of rapid genetics-based assays has decreased
47 diagnostic time to as little as 2 hours through the detection of specific resistance
48 conferring mutations e.g. the Cepheid Xpert® MTB/RIF test (2,3). However, assay bias
49 towards specific genic regions can result in misdiagnosis of resistance, the
50 prescription of ineffective treatment regimens and subsequent spread of multi-drug
51 resistant disease, as seen during an MDR outbreak in Eswatini (4–6). Furthermore,
52 detection of rifampicin resistance is used to infer MDR-TB epidemiologically as
53 rifampicin resistance tends to coincide with resistance to isoniazid (7). While this
54 *modus operandi* is successful at pragmatically identifying potential MDR cases quickly

55 and effectively, it is not generally true that a single path exists for developing MDR or
56 extensively drug resistant TB (XDR = MDR/RR + resistance to at least one
57 fluoroquinolone and either bedaquiline or linezolid).

58

59 Whole-genome sequencing (WGS) has the potential to reveal the entirety of
60 the *M. tuberculosis* genetic resistance landscape for any number of drugs
61 simultaneously whilst enabling a more rapid turnaround time and reduction in cost
62 compared to DST culture-based methods (8). However, the success of WGS as a
63 diagnostic tool wholly depends on there being a comprehensive and accurate
64 catalogue of resistance-conferring mutations for each drug. Recent advances have
65 shown that genotypic predictions of resistance correlate well with DST measurements
66 for first-line drugs (7). However, the mechanisms of resistance to second-line drugs
67 along with the new and re-purposed drugs (NRDs) are less well understood despite
68 their increased administration in clinics as MDR cases climb(1,9).

69

70 To address these shortcomings, the Comprehensive Resistance Prediction for
71 Tuberculosis: an International Consortium (CRyPTIC) has collected *M. tuberculosis*
72 clinical isolates worldwide to survey the genetic variation associated with resistance
73 to 13 antitubercular drugs, specifically the first-line drugs rifampicin, isoniazid,
74 ethambutol, the second-line drugs amikacin, kanamycin, rifabutin, levofloxacin,
75 moxifloxacin, ethionamide, and the new and re-purposed drugs bedaquiline,
76 clofazimine, delamanid and linezolid. Here, we introduce and describe these data in
77 the form of an open-access compendium of 15,211 isolates, each of which has had its
78 genomic sequence determined and DST profile measured (10). This compendium is
79 the largest drug screening effort to date for *M. tuberculosis* in a ‘one isolate – one

80 microscale assay' format across defined compound concentration ranges. The
81 presented dataset forms the backbone for several studies being put forth by the
82 consortium to achieve its ultimate aim (11–15). By being fully open-access, it is hoped
83 that this compendium will prove an invaluable resource to accelerate and improve
84 antimicrobial resistance (AMR) diagnostic development for TB, both by the enrichment
85 of mutation catalogues for WGS resistance prediction and the identification of
86 important diagnostic gaps and drug resistance patterns.

87

88

89 **Methods**

90 ***Ethics***

91 Approval for the CRyPTIC study was obtained by Taiwan Centers for Disease
92 Control IRB No. 106209, University of KwaZulu Natal Biomedical Research Ethics
93 Committee (UKZN BREC) (reference BE022/13) and University of Liverpool Central
94 University Research Ethics Committees (reference 2286), Institutional Research
95 Ethics Committee (IREC) of The Foundation for Medical Research, Mumbai (Ref nos.
96 FMR/IEC/TB/01a/2015 and FMR/IEC/TB/01b/2015), Institutional Review Board of
97 P.D. Hinduja Hospital and Medical Research Centre, Mumbai (Ref no. 915-15-CR
98 [MRC]), scientific committee of the Adolfo Lutz Institute (CTC-IAL 47-J / 2017) and in
99 the Ethics Committee (CAAE: 81452517.1.0000.0059) and Ethics Committee review
100 by Universidad Peruana Cayetano Heredia (Lima, Peru) and LSHTM (London, UK).

101

102 ***Sample collection***

103 Participating collection centres varied in their isolate collection approaches and
104 timescales (e.g. longitudinal sampling, rolling patient visits, biobank stocks), but the

105 consortium collectively aimed to oversample for *M. tuberculosis* isolates with drug
106 resistance and multi-drug resistance. A standard operating protocol for sample
107 processing was defined by CRyPTIC as previously described and is discussed in more
108 detail below in relevant sub-sections (10,11).

109

110 **Plate assay**

111 The CRyPTIC consortium designed two versions of the Sensititre MYCOTB
112 plate (Thermo Fisher Scientific Inc., USA) named the “UKMYC5” and “UKMYC6”
113 microtitre plates (10,11). These plates contain five to ten doubling dilutions of 13
114 antibiotics (rifampicin (RIF), rifabutin (RFB), isoniazid (INH), ethambutol (EMB),
115 levofloxacin (LEV), moxifloxacin (MXF), amikacin (AMI), kanamycin (KAN),
116 ethionamide (ETH), clofazimine (CFZ), linezolid (LZD), delamanid (DLM), and
117 bedaquiline (BDQ)). Delamanid and bedaquiline were provided by Otsuka
118 Pharmaceutical Co., Ltd. and Janssen Pharmaceutica respectively. The UKMYC5
119 plate also contained para-aminosalicylic acid (PAS), but the MICs were not
120 reproducible and hence it was excluded from the UKMYC6 plate design and is not
121 included in any subsequent analysis (10).

122 A standard operating protocol for sample processing was defined by CRyPTIC
123 as previously described (10,11). Clinical samples were sub-cultured using 7H10 agar
124 plates, Lowenstein-Jensen tubes or MGIT tubes. Bacterial cell suspensions (0.5
125 McFarland standard, saline Tween) prepared from (no later than) 14-day old colonies
126 were diluted 100X in 10 ml enriched 7H9 broth prior to plate inoculation. A semi-
127 automated Sensititre Autoinoculator (Thermo Fisher, Scientific Inc., USA) was used to
128 inoculate 100 μ l prepared cell suspensions (1.5×10^5 CFU/ml [5×10^4 CFU/ml - $5 \times$
129 10^5 CFU/ml]) into each well of a UKMYC5/6 microdilution plate. The plate was sealed

130 and incubated for 14 days at 37°C. Quality control runs were performed periodically
131 using *M. tuberculosis* H37Rv ATCC 27294, which is sensitive to all drugs on the plates.

132

133 ***Minimum Inhibitory Concentration (MIC) measurements***

134 Minimum inhibitory concentrations (MICs) for each drug were read after
135 incubation for 14 days by a laboratory scientist using a Thermo Fisher Sensititre™
136 Vizion™ digital MIC viewing system (10). The Vizion apparatus was also used to take
137 a high contrast photograph of the plate with a white background, from which the MIC
138 was measured again using the Automated Mycobacterial Growth Detection Algorithm
139 (AMyGDA) software (16). The AMyGDA algorithm was specifically developed to
140 automate and perform quality control of MIC measurements, and to facilitate machine
141 learning studies within the consortium. AMyGDA detects the boundaries of each well
142 using a Hough transform for circles and measures growth as the number of dark pixels
143 within the area contained by this boundary.

144 All images where the MICs measured by Vizion and AMyGDA were different
145 were uploaded to a citizen science project, BashTheBug, on the Zooniverse platform
146 (17). Each image was then classified by ≥11 volunteers and the median classification
147 taken. MICs were then classified as high (at least two methods concur on the MIC),
148 medium (either a scientist recorded a MIC measurement using Vizion but did not store
149 the plate picture, or Vizion and AMyGDA disagree and there is no BashTheBug
150 measurement), or low (all three methods disagree) quality.

151 To ensure adequate data coverage for *this* study, we took the MIC from the
152 Vizion reading provided by the trained laboratory scientist if it was annotated as having
153 medium or low quality.

154

155 ***Binary phenotype classification***

156 Binary phenotypes (resistant/susceptible) were assigned from the MICs by
157 applying epidemiological cut-off values (11); samples with MICs at or below the
158 ECOFF are, by definition, wild-type and hence assigned to be susceptible to the drug
159 in question (11). Samples with MICs above the ECOFF are therefore classified as
160 resistant (Fig. S1, Table S1). Please see (11) for the body of work supporting the use
161 of the ECOFF relative to the compendium isolates and supplemental Table S1 for the
162 ECOFFs for each drug tested.

163

164

165 ***Genomic data processing and variant calling***

166 Short-read, paired end libraries were sequenced on Illumina machines and the
167 resulting FASTQ files were processed using the bespoke pipeline Clockwork (v0.8.3,
168 github.com/iqbal-lab-org/clockwork, (18)). Briefly, all raw sequencing files were
169 indexed into a relational database with which Clockwork proceeds. Human,
170 nasopharyngeal flora and human immunodeficiency virus related reads were removed
171 and remaining reads were trimmed (adapters and low quality ends) using Trimmomatic
172 and mapped with BWA-MEM to the *M. tuberculosis* H37Rv reference genome
173 (NC000962.3) (19,20). Read duplicates were removed. Genetic variants were called
174 independently using Cortex and SAMtools, two variant callers with orthogonal
175 strengths (SAMtools a high sensitivity SNP caller, and Cortex a high specificity SNP
176 and indel caller) (21,22). The two call sets were merged to produce a final call set,
177 using the Minos adjudication tool to resolve loci where the two callers disagreed, by
178 remapping reads to an augmented genome containing each alternative allele (23).
179 Default filters of a minimum depth of 5x, a fraction of supporting reads of 0.9 (minos)

180 and a genotype confidence percentile (GCP) filter of 0.5 were applied. The GCP filter
181 is a normalised likelihood ratio test, giving a measure of confidence in the called allele
182 compared with the other alternatives, and is described in (23). This produced one
183 variant call format (VCF) file per sample, each only describing positions where that
184 sample differed from the reference.

185

186 These filtered VCFs were then combined, to produce a single non-redundant
187 list of all variants seen in the cohort. All samples were then processed a second time
188 with Minos, remapping reads to a graphical representation of all the segregating
189 variation within the cohort, generating VCF files which had an entry at all variable
190 positions (thus for all samples, most positions would be genotyped as having the
191 reference allele). These “regenotyped” VCFs were later used to calculate pairwise
192 distances (see below).

193

194 To remove untrustworthy loci, a genome mask was applied to the resulting VCF
195 files (regions identified with self-blast matches in (24) comprising of 324,971 bp of the
196 reference genome). Furthermore, positions with less than 90% of total samples
197 passing default Clockwork/Minos variant call filters (described above) were filtered out,
198 comprising 95,703 bp of the genome, of which 55,980 bp intersect with the genome
199 mask.

200

201 ***Resistance prediction using a genetic catalogue***

202 A hybrid catalogue of genetic variants associated with resistance to first- and
203 second- line drugs based on existing catalogues was created and can be found at
204 github.com/oxfordmmm/tuberculosis_amr_catalogues/blob/public/catalogues/NC_00

205 0962.3/NC_000962.3_CRyPTIC_v1.311_GARC1_RUS.csv (7,25). We specifically
206 did not use the recent WHO catalogue to avoid circularity and over-training, as that
207 catalogue was developed (via prior literature, expert rules and a heuristic algorithm)
208 based partially on these isolates (26)).
209 The resulting VCF file for each isolate (see “*Genomic data processing and variant*
210 *calling*” section above) was compared to the genetic catalogue to determine the
211 presence or absence of resistance-associated mutations for eight drugs: rifampicin,
212 isoniazid, ethambutol, levofloxacin, moxifloxacin, amikacin, kanamycin and
213 ethionamide. We did not apply the approach used in (7) to make a prediction if a novel
214 mutation was detected in a known resistance gene, as we simply wanted to measure
215 how well a pre-CRyPTIC catalogue could predict resistance in the compendium.
216 These results (found in PREDICTIONS.csv, see “Data availability” section for access)
217 were then compared to the binary phenotypes (see “Binary phenotype classification”
218 section for how these were defined) with the following metrics calculated: TP: the
219 number of phenotypically resistant samples that are correctly identified as resistant
220 (“true positives”); FP, the number of phenotypically susceptible samples that are
221 falsely identified as resistant (“false positives”); TN, the number of phenotypically
222 susceptible samples that are correctly identified as susceptible (“true negatives”); FN,
223 the number of phenotypically resistant samples that are incorrectly identified as
224 susceptible (“false negative”); VME, very major error rate (false-negative rate), 0-1;
225 ME, major error rate (false-positive rate), 0-1; PPV, positive predictive value, 0-1; NPV,
226 negative predictive value.
227
228
229

230 ***Phylogenetic tree construction***

231 A pairwise genetic distance matrix was constructed for 15,211 isolates by
232 comparing pairs of regenotyped VCF files (see “*Genomic data processing and variant*
233 *calling*” section above for more details). A neighbourhood-joining tree was constructed
234 from the distance matrix using *quicktree* (27). Tree visualisation and annotation was
235 performed using the R library *ggtree* (28). *M. tuberculosis* lineages were assigned
236 using Mykrobe and are represented by the coloured dots at the branch termini of the
237 tree (23). For isolates that had ‘mixed’ lineage classification (*i.e.*, 2 lineages were found
238 present in the sample by Mykrobe, $n = 225$, 1.5%), the first of the two lineages was
239 assigned to the isolate. *ggtree* was also used to construct the trees depicting
240 bedaquiline, clofazimine and delamanid resistant isolates.

241

242 ***The Data***

243 All data can be found at [ftp.ebi.ac.uk/pub/databases/cryptic/reuse/](ftp://ftp.ebi.ac.uk/pub/databases/cryptic/reuse/). The FTP
244 site contains two top level directories: “reuse” and “reproducibility”. In total, the
245 compendium contains data entries for 15,211 isolates. Note that various filtering
246 criteria have been applied in both this study and other CRyPTIC studies and thus final
247 isolate numbers presented across the publications will vary.

248

249 “*reuse*” directory

250 We point the reader to this directory to gain access to CRyPTIC project data.
251 “CRyPTIC_reuse_table_20221019.csv” contains genotypic and phenotypic data
252 relating to the figures and summaries listed in this manuscript and is what we present
253 as a general use reference table for most future projects. It includes binary phenotypes
254 (R/S), MICs, phenotype quality metrics, and ENA sample IDs for 12,288 compendium

255 isolates (see “Quality assurance of the minimum inhibitory concentrations for 13 drugs”
256 section below in Results for filters applied to obtain this final set of isolated). It also
257 includes file paths to each isolate’s VCF file and ‘regenotyped’ VCF file (VCF files
258 which have an entry at all variable positions, see “Genomic data processing and
259 variant calling” section above for more).

260

261 *“reproducibility” directory*

262 This directory contains the data used for multiple CRyPTIC project publications
263 referenced throughout this manuscript. As stated above, each project has taken
264 slightly different subsets of this data as documented in those papers. For example,
265 see how tables such as “MUTATIONS.csv” and “GENOTYPES.csv” were used and
266 filtered, (along with others) in this study to obtain the reuse file
267 “CRyPTIC_reuse_table_20221019.csv” in Figure 1. Again, for optimal use of
268 CRyPTIC data in your own project, please refer to
269 “CRyPTIC_reuse_table_20221019.csv” in the “reuse” directory. All data for this study
270 were analysed and visualised using either R or python3 libraries and packages. See
271 github.com/kerrimalone/Brankin_Malone_2022 for codebase.

272

273

274

275

276

277

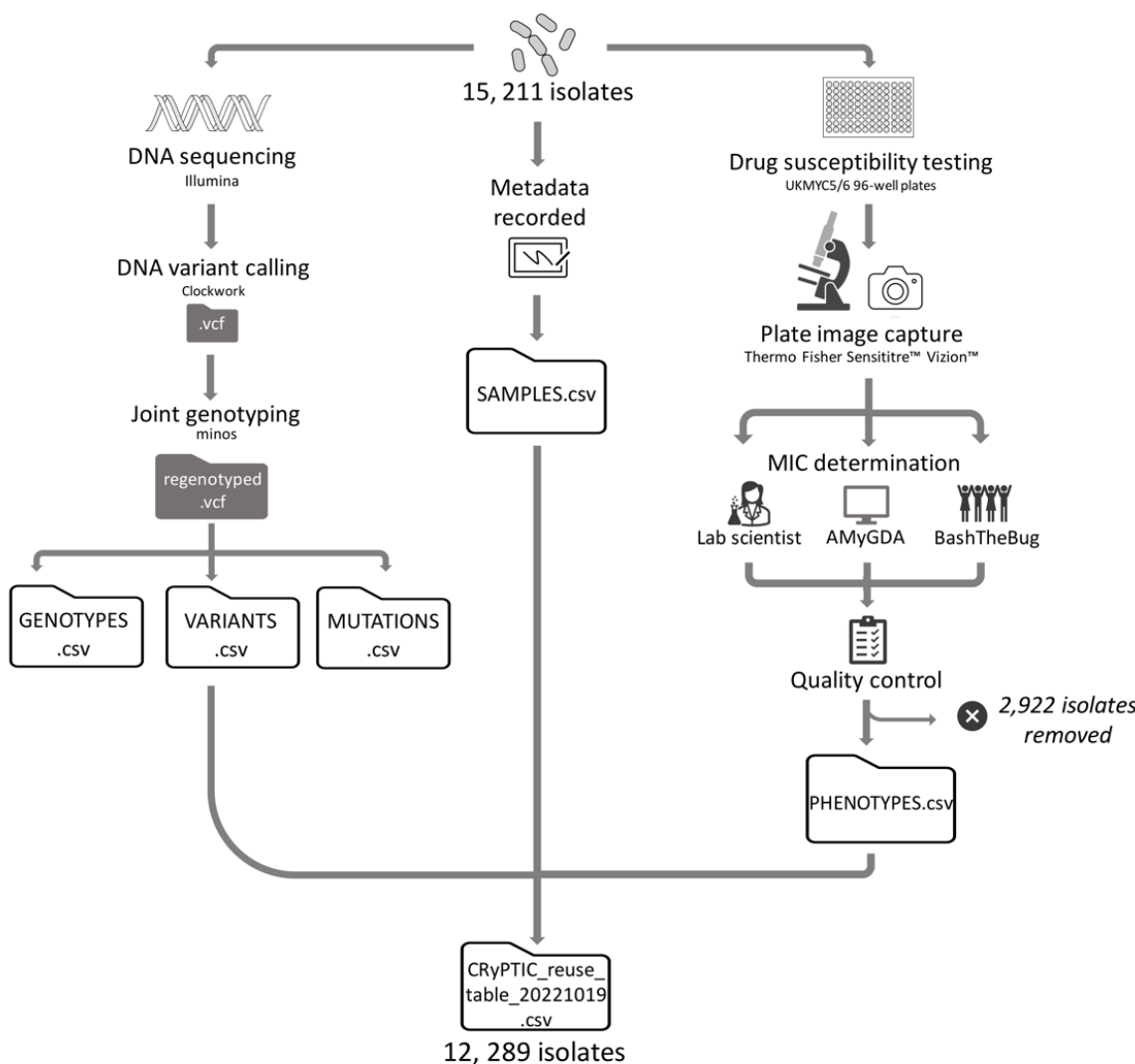
278

279

280 Results

281 **15,211 *M. tuberculosis* clinical isolates**

282 The CRyPTIC compendium contains 15,211 isolates for which both genomic
283 and phenotypic data was collected by 23 of the partner countries across the continents
284 of Asia, Africa, South America and Europe. An overview of the processing of the
285 isolates is presented in Figure 1, and for a full description please see Methods.



286

287 **Figure 1: Processing sequencing and MIC data for 15,211 *M. tuberculosis* isolates**

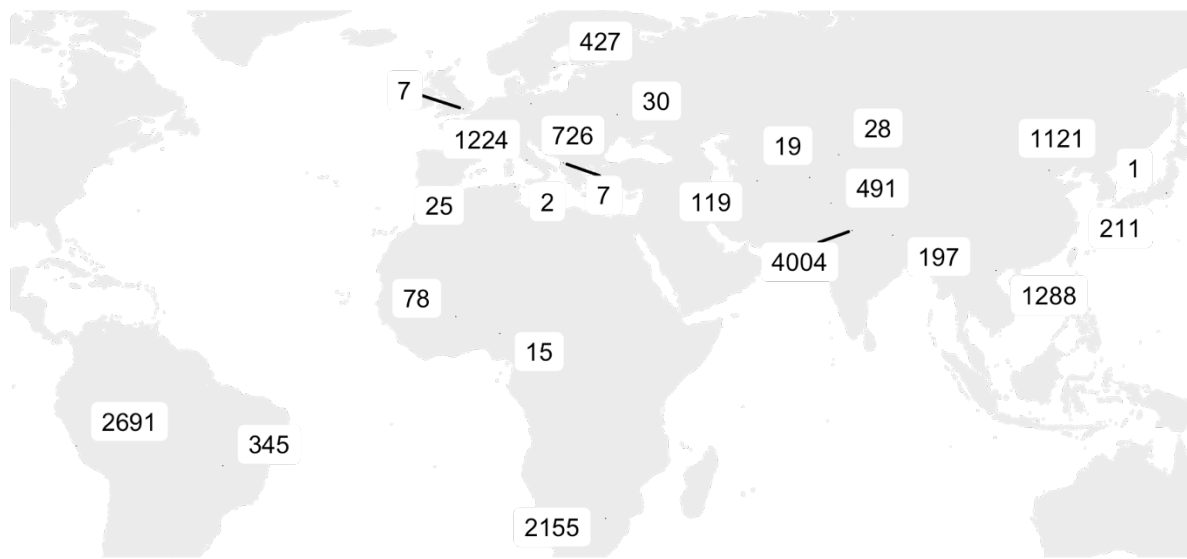
288 Briefly: Each isolate was DNA sequenced using an Illumina machine and plated onto 96
289 well plates (UKMYC5/6) containing 5-10x doubling dilutions of 13 antitubercular drugs for drug
290 susceptibility testing. Associated metadata (including country of origin and processing laboratory)
291 was recorded. DNA variant calling and analysis was performed using Clockwork and minos. After
292 14 days, MIC measurements were measured by a trained scientist using Vizion, and the plate was

photographed to measure the MIC using the automated AMyGDA software and citizen scientists from BashTheBug. After quality control procedures, phenotypic MIC data for 2,922 isolates were removed. The compendium therefore contains 15,211 isolates with whole genome sequencing data, 12,289 of which have matched phenotypic data, presented in "CRyPTIC_reuse_table_20211019.csv" via an FTP site (see methods). The data tables GENOTYPES.csv, VARIANTS.csv, MUTATIONS.csv, SAMPLES.csv and PHENOTYPES.csv used for the analyses presented in this manuscript are also accessible via the FTP site (see methods).

301
302
303

304

305 The 15, 211 isolates originated from 23 different countries (Fig. 2). The largest
306 number of isolates were contributed by India ($n = 4,004$), Peru ($n = 2,691$), South
307 Africa ($n = 2,155$), Vietnam ($n = 1,288$) and China ($n = 1,121$).



308

309

Figure 2: Geographical distribution of CRyPTIC *M. tuberculosis* clinical isolates.

The total number of isolates contributed by each country is depicted. Where labels overlap, labels are exploded and lines are used to indicate country of origin, from left to right: UK, Albania, India. Where the origin of an isolate was not known, the collection site identity was assigned (this occurred for 269 isolates in Germany, 17 isolates in India, 6 isolates in Peru, 885 isolates in Italy,

315 510 isolates in South Africa, 357 isolates in Sweden, 208 isolates in Taiwan, 1 isolate in Brazil and
316 4 isolates in the UK).

317

318

319

320 Lineage assignment revealed that 99.7% of the 15,211 isolates belong to the
321 four main *M. tuberculosis* lineages (L1-L4). The pie-charts in supplemental Figure S2
322 show the proportion of isolates amongst the different lineages (Table S2) and sub-
323 lineages (Table S3) for each location. Like previous studies, we see a strong
324 association between geolocation and lineage (Pearson's chi-squared test, $p < 2.2e-$
325 16, Fig. S3) (29,30). The phylogenetic tree in supplemental figure S4 further highlights
326 the strong population structure of this collection of isolates, with isolates clustering
327 according to lineage. Typically under-sampled in current databases and biobanks, the
328 L3 isolates in this study represent the largest collection to date (31).

329

330 Although these 15,211 *M. tuberculosis* isolates were plated to determine their
331 MICs to 13 antitubercular drugs, regular quality assurance checks detected problems
332 with plate inoculation and reading in two laboratories. Therefore, 2,922 isolates were
333 removed from the dataset, leaving a total of 12,289 isolates with matched phenotypic
334 and genotypic data for further analysis (Fig.1). Due to wells being skipped and other
335 phenomena that prevent an MIC being measured, 88.1% of the isolates had a
336 phenotype for all 13 drugs on the plate. For each drug, the number of isolates with an
337 MIC measurement, and the associated quality of the reading, is presented in Table 1.

338

339

340

MEASUREMENTS	MIC	HIGH QUALITY	MEDIUM QUALITY	LOW QUALITY
INH	12070	9519	1351	1200
RIF	12099	8955	1356	1788
EMB	12158	7506	1355	3297
LEV	12163	7774	1354	3035
MXF	12194	6785	1353	4056
AMI	12072	8973	1350	1749
KAN	12130	9333	1355	1442
BDQ	12068	8536	1355	2177
CFZ	12049	7763	1352	2934
DLM	11927	8095	1349	2483
LZD	12189	7141	1355	3693
ETH	12132	8821	1355	1956
RFB	12150	10042	1352	756
TOTAL	157401	109243	17592	30566

341

342 **Table 1: Quality metrics for phenotype data** Stated for each drug is the total number of
343 MIC measurements stratified into “high” quality (at least two MIC measurement methods agree),
344 “medium” quality (either Vizion and AMyGDA disagree, or the scientist recorded a MIC
345 measurement using Vizion but did not store the plate picture) or “low” quality (all three MIC
346 measurements methods disagree) phenotype classifications as described in Methods. Drug
347 acronyms: INH = isoniazid, RIF = rifampicin, EMB = ethambutol, LEV = levofloxacin, MXF =
348 moxifloxacin, AMI = amikacin, KAN = kanamycin, BDQ = bedaquiline, CFZ = clofazimine, DLM =
349 delamanid, LZD = linezolid, ETH = ethionamide, RFB = rifabutin.

350

351 **Resistance classification and distribution**

352 Unsurprisingly, given its size and bias toward the collection of resistant isolates,
353 resistance to each of the 13 drugs is represented within the compendium (Fig. 3a).
354 The drugs with the highest percentage of resistant isolates are the first line drugs
355 isoniazid and rifampicin (49.0% and 38.7% respectively). Of the second line drugs,
356 levofloxacin had the highest proportion of resistant isolates in the dataset (17.6%) and
357 amikacin the lowest (7.3%). A low proportion of isolates were resistant to the NRDs,
358 bedaquiline (0.9%), clofazimine (4.4%), delamanid (1.6%) and linezolid (1.3%).

359

360 Of the 12,289 isolates with matched phenotypic and genotypic data, 6,814
361 (55.4%) were resistant to at least one drug (Fig. 3b). For the purpose of describing
362 five broader resistance categories present in the dataset, we assumed that all MICs
363 that could not be read had susceptible phenotypes. These five resistance categories
364 comprise: isoniazid and rifampicin susceptible with resistance to another
365 antitubercular drug, isoniazid resistant but rifampicin susceptible, RR/MDR, pre-XDR
366 (RR/MDR + fluoroquinolone resistance), and XDR (RR/MDR + fluoroquinolone
367 resistance + resistance to a group A agent: bedaquiline or linezolid)). Consequently,
368 the calculated prevalence of MDR, XDR etc. in the dataset (Fig. 3) are likely under-
369 estimates. Of the isolates resistant to one or more drugs, 22.8% were resistant to
370 isoniazid and not rifampicin, 68.8% were either RR or MDR and 8.4% were resistant
371 to at least one antitubercular drug, but *not* isoniazid or rifampicin (Fig. 3b). Of the
372 RR/MDR isolates, 38.8% were pre-XDR and 3.0% were XDR. Two of the XDR isolates
373 returned a resistant phenotype to all 13 of the drugs assayed (Table S5) and therefore
374 could be reasonably described as totally drug resistant (TDR). One such isolate
375 belonged to L4 and was contributed by South Africa, and the other belonged to L2 with
376 an unknown country of origin contributed by Sweden.

377

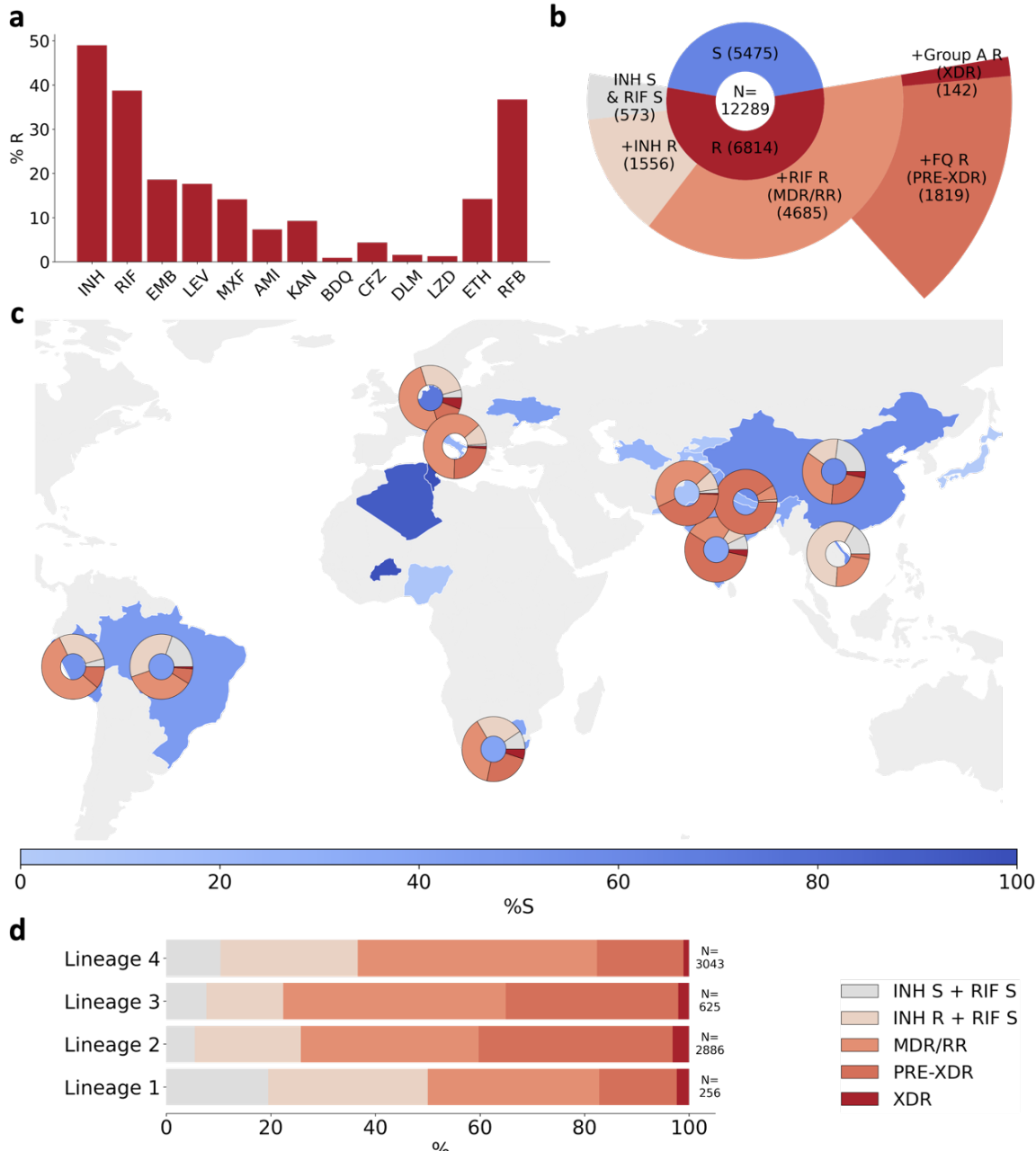
378 The proportion of drug susceptible isolates collected differed between
379 countries, as not all laboratories oversampled for resistance (Fig. 3c). In countries that
380 contributed more than 100 resistant isolates, each of the broad phenotypic resistance
381 categories in Fig. 3b were seen except for Peru, Vietnam and Nepal which did not
382 contribute any XDR isolates (Fig. 3c). Vietnam and Brazil sampled a high proportion
383 of non-MDR/RR resistant phenotypes; 73.9% and 55.1% of resistant isolates
384 contributed by these countries, respectively, were neither MDR nor RR. For Nepal and

385 India, an especially high proportion of the MDR/RR isolates contributed were
386 fluoroquinolone resistant (92.9% and 69.8% respectively), which has been previously
387 observed for this geographical region (32,33).

388

389 Of the 6814 resistant isolates, 256 were from L1, 2886 were from L2, 625 were
390 from L3 and 3043 were from L4. All five broader categories of resistance were
391 represented in the four major *M. tuberculosis* lineages (Fig. 3d). We note that the
392 relative proportions of resistance categories will have been influenced by the different
393 local sampling approaches since lineage distributions are typically geographically
394 distinct (Fig. S2). Bearing this in mind, we observe that in the compendium, L3 isolates
395 contained the most MDR/RR isolates as a proportion of resistant isolates (77.6%), L2
396 isolates contained the most pre-XDR isolates as a proportion of MDR/RR isolates
397 (54.2%) and L2 contained the most XDR isolates as a proportion of MDR/RR isolates
398 (4.7%).

399



400
401 **Figure 3: Drug phenotype data for the CRyPTIC compendium** a) Frequency of
402 resistance to each of 13 drugs in the CRyPTIC dataset. The total number of isolates with a binary
403 phenotype (of any quality) for the corresponding drug is presented in Table 1. b) Phenotypes of
404 12,289 CRyPTIC isolates with a binary phenotype for at least one drug. c) Geographical
405 distribution of phenotypes of 12,289 CRyPTIC isolates. Intensity of blue shows the percentage of
406 isolates contributed that were categorised as susceptible to all 13 drugs. Donut plots show the
407 proportions of resistant phenotypes identified in (b) for countries contributing ≥ 100 isolates with
408 drug resistance. d) Proportions of resistance phenotypes in the 4 major *M. tuberculosis* lineages.
409 N is the number of isolates of the lineage called resistant to at least one of the 13 drugs. Drug
410 acronyms: INH = isoniazid, RIF = rifampicin, EMB = ethambutol, LEV = levofloxacin, MXF =
411 moxifloxacin, AMI = amikacin, KAN = kanamycin, BDQ = bedaquiline, CFZ = clofazimine, DLM =
412 delamanid, LZD = linezolid, ETH = ethionamide, RFB = rifabutin.

413

414 ***Co-occurrence of drug resistance amongst the CRyPTIC isolates***

415 As we measured MICs to 13 drugs in parallel, we can ask whether, and how
416 often, co-occurrence of drug resistance occurs amongst the isolates. We found
417 isolates with all possible two-drug resistant combinations in this dataset (Fig. 4a, Table
418 S6). With the exception of correlations between drugs in the same class (rifabutin vs
419 rifampicin, moxifloxacin vs levofloxacin), Isoniazid resistance was the most strongly
420 associated with resistance to each of the other drugs. Resistance to any of the drugs
421 was also strongly associated with resistance to rifampicin. Of the second line drugs,
422 levofloxacin and moxifloxacin were more commonly seen as a second resistant
423 phenotype than the injectable drugs kanamycin and amikacin.

424

425 Resistance to both drugs in the aminoglycoside class was common in the
426 dataset; 90.4% of amikacin resistant isolates were also resistant to kanamycin
427 although significantly fewer kanamycin resistant isolates were resistant to amikacin
428 (72.0%, $p < 0.00001$) (Fig. 4a). In a similar fashion, a smaller proportion of rifampicin
429 resistant isolates were resistant to rifabutin than rifabutin resistant isolates that were
430 resistant to rifampicin (91.3%, 96.8%, $p < 0.00001$) while a smaller proportion of
431 levofloxacin resistant isolates were resistant to moxifloxacin than moxifloxacin
432 resistant isolates that were resistant to levofloxacin (78.5%, 97.6%, $p < 0.00001$).

433

434 Differences in drugs of the same class are also well documented by *in vitro*
435 studies (34–36).

436

437 Isolates resistant to the NRDs bedaquiline, clofazimine, delamanid and linezolid
438 were most likely to also be resistant to isoniazid, followed by rifampicin and rifabutin.
439 The NRDs were less commonly seen as a second resistance phenotype and the
440 smallest proportional resistance combinations involved the NRDs (e.g. 1.5% of
441 isoniazid resistant isolates were bedaquiline resistant). Within the NRDs however, co-
442 occurrence of resistance was proportionally higher; bedaquiline, linezolid and
443 delamanid resistance was commonly seen with clofazimine resistance (52.4%, 34.2%
444 and 26.3% of isolates having co-resistance with clofazimine respectively).

445

446 ***Additional antibiotic resistance in isolates with non-MDR or MDR phenotypic***
447 ***backgrounds***

448 To further investigate drug resistance patterns amongst the isolates, we
449 examined in more detail the correlation structure of phenotypes by conditioning on
450 different resistance backgrounds including isoniazid and rifampicin susceptible,
451 isoniazid resistant and rifampicin susceptible, rifampicin resistant and isoniazid
452 susceptible, MDR, pre-XDR and XDR (Fig. 4b-f). We found that a greater proportion
453 of isolates that were susceptible to isoniazid and rifampicin were resistant to the
454 second line drugs levofloxacin (24.1%), kanamycin (18.1%), moxifloxacin (13.7%),
455 and amikacin (8.9%) than the first line drug ethambutol (3.8%) (Fig. 4b). The proportion
456 of isolates resistant to clofazimine or levofloxacin was particularly high (32.9% and
457 24.1%, respectively), and more isolates were resistant to these two drugs than
458 ethambutol in an isoniazid resistant and rifampicin susceptible background but not in
459 MDR/RR isolates (Fig. 4c-f).

460

461 MDR/RR isolates were most commonly resistant (excluding rifabutin) to the first
462 line drug ethambutol (46.3%), closely followed by levofloxacin (41.4%). As expected,
463 the proportion of fluoroquinolone resistance was higher in MDR/RR isolates than non-
464 MDR isolates (37) and we found a greater proportion of isolates were resistant to
465 levofloxacin than moxifloxacin, a pattern seen in all other backgrounds (Fig. 4c-f). For
466 the aminoglycosides, a greater percentage of MDR/RR isolates were kanamycin
467 resistant (21.8%) than amikacin resistant (18.1%), a trend seen in all other
468 backgrounds.

469

470 For isolates with an XDR phenotype, a higher proportion were resistant to
471 linezolid than bedaquiline (66.7% compared to 44.6%) and 11.3% of XDR isolates
472 were resistant to both bedaquiline and linezolid (Fig. 4f). XDR isolates were also
473 resistant to the other NRDs, clofazimine (41.3%) and delamanid (18.8%). In non-XDR
474 backgrounds the most common NRD resistance seen was clofazimine (Fig. 4b-e).

475

476

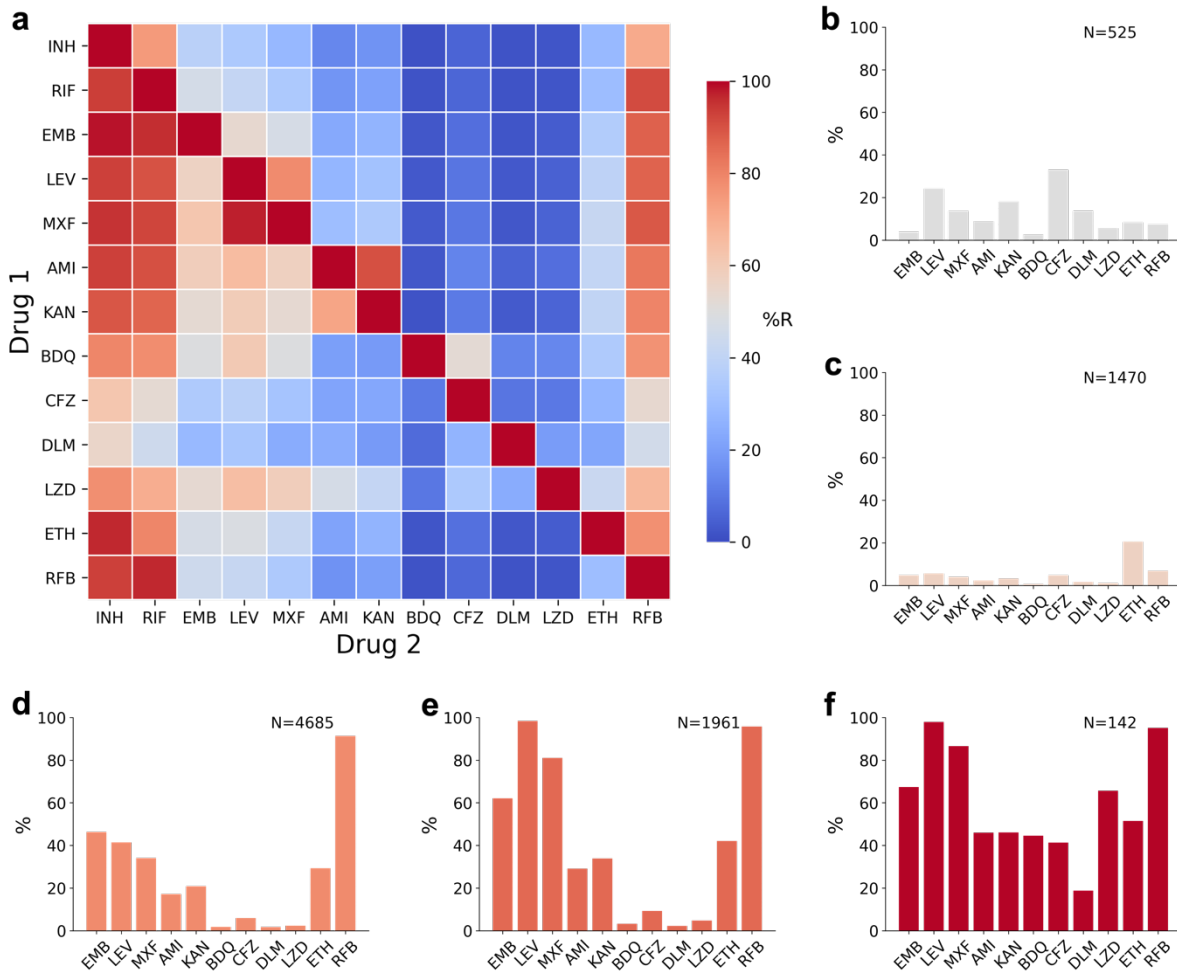


Figure 4: Co-occurrence of resistance to one drug conditional on resistance to another drug, or to resistance background. **a)** The heatmap shows the probability of an isolate being resistant to Drug 2 if it is resistant to Drug 1, percentages are given in Table S4. **(b-g)** Percentage of isolates that are resistant to another of the 13 drugs in a background of **(b)** isoniazid susceptible + rifampicin susceptible (but resistant to at least one other antitubercular drug), **(c)** isoniazid resistant + rifampicin susceptible, **(d)** MDR/RR, **(e)** Pre-XDR, **(f)** XDR. Only samples with definite phenotypes for RIF in MDR backgrounds and RIF and INH in non-MDR backgrounds and the additional drug are included. Drug acronyms: INH = isoniazid, RIF = rifampicin, EMB = ethambutol, LEV = levofloxacin, MXF = moxifloxacin, AMI = amikacin, KAN = kanamycin, BDQ = bedaquiline, CFZ = clofazimine, DLM = delamanid, LZD = linezolid, ETH = ethionamide, RFB = rifabutin.

Genetic-based predictions of resistance

To establish a baseline measure of how well resistance and susceptibility could

be predicted based on the state of the art prior to the CRyPTIC project, we compared

genetic-based predictions of susceptibility and resistance to the binary phenotypes

495 derived from MICs for eight drugs and for all isolates in this compendium (Table 2).
496 Since these data were not collected prospectively or randomly, but indeed are
497 enriched for resistance, the calculated error rates are not representative of how well
498 such a method would perform in routine clinical use. The results were broadly in line
499 with prior measurements on a smaller (independent) set (23). The hybrid catalogue
500 does not make predictions for rifabutin, linezolid, bedaquiline, delamanid or
501 clofazimine; indeed, this is one of the main aims of the consortium and new catalogues
502 published by CRyPTIC and the WHO will begin to address this shortcoming (Fig. 5)
503 (26).

504

505

506

507 Table 3 shows the top mutations found amongst isolates phenotypically
508 resistant to first- and second- line drugs. As expected, *rpoB* S450L was the most
509 prevalent mutation associated with rifampicin resistance and *katG* S315T was the
510 most prevalent mutation associated with isoniazid resistance. Mutations in *gyrA*
511 dominate amongst fluoroquinolone resistant isolates; D94G and A90V are the two
512 most frequently occurring mutations for levofloxacin and moxifloxacin.

513

514

515

516

517

518

519

520

	TP	FP	TN	FN	VME	ME	PPV	NPV
INH	5493	142	5622	224	0.039	0.025	0.961	0.975
RIF	4535	435	6669	107	0.023	0.061	0.977	0.939
EMB	1919	513	6702	111	0.055	0.071	0.945	0.929
LEV	1689	255	8104	184	0.098	0.031	0.902	0.969
MXF	1358	504	9022	160	0.105	0.053	0.895	0.947
AMI	632	84	10117	163	0.205	0.008	0.795	0.992
KAN	735	124	9043	197	0.211	0.014	0.789	0.986
ETH	971	114	9183	511	0.345	0.012	0.655	0.988

521

522 **Table 2: Predicting phenotypic resistance using genetics**

523 Statistics on how well phenotypic resistance could be predicted using a standard resistance
524 catalogue that predates the CRyPTIC project. TP: the number of phenotypically resistant samples
525 are that correctly identified as resistant ("true positives"); FP, the number of phenotypically
526 susceptible samples that are falsely identified as resistant ("false positives"); TN, the number of
527 phenotypically susceptible samples that are correctly identified as susceptible ("true negatives");
528 FN, the number of phenotypically resistant samples that are incorrectly identified as susceptible
529 ("false negative"); VME, very major error rate (false-negative rate), 0-1; ME, major error rate (false-
530 positive rate), 0-1; PPV, positive predictive value, 0-1; NPV, negative predictive value, 0-1. Drug
531 acronyms: INH = isoniazid, RIF = rifampicin, EMB = ethambutol, AMI = amikacin, KAN =
532 kanamycin, LEV = levofloxacin, MXF = moxifloxacin, ETH = ethionamide.

533

534

535

536

537

538

539

540

541

542

543

544

545

546

	GENE	VARIANT	n	%
Rifampicin	<i>rpoB</i>	S450L	2914	62.2
	<i>rpoB</i>	D435V	506	10.8
	<i>rpoB</i>	H445D	202	4.3
	<i>rpoB</i>	H445Y	147	3.1
	<i>rpoB</i>	D435Y	112	2.4
Isoniazid	<i>katG</i>	S315T	3668	70.0
	<i>fabG1</i>	c-15t	829	15.8
	<i>fabG1</i>	g-17t	176	3.4
	<i>fabG1</i>	t-8c	154	2.9
	<i>inhA</i>	I194T	56	1.1
Ethambutol	<i>embB</i>	M306V	1131	50.0
	<i>embB</i>	M306I	1001	44.3
	<i>embB</i>	Q497R	449	19.9
	<i>embB</i>	G406A	164	7.2
	<i>embB</i>	G406D	105	4.6
Kanamycin	<i>rrs</i>	a1401g	660	58.9
	<i>eis</i>	c-14t	70	6.2
	<i>eis</i>	g-10a	53	4.7
Amikacin	<i>rrs</i>	a1401g	660	74.7
	<i>rrs</i>	g1484t	7	0.8
Levofloxacin	<i>gyrA</i>	D94G	783	36.5
	<i>gyrA</i>	A90V	487	22.7
	<i>gyrA</i>	D94N	157	7.3
	<i>gyrA</i>	D94A	133	6.2
	<i>gyrA</i>	S91P	92	4.3
Moxifloxacin	<i>gyrA</i>	D94G	783	45.4
	<i>gyrA</i>	A90V	487	28.2
	<i>gyrA</i>	D94N	157	9.1
	<i>gyrA</i>	D94A	133	7.7
	<i>gyrA</i>	D94Y	70	4.1
Ethionamide	<i>fabG1</i>	c-15t	829	48.0
	<i>fabG1</i>	L203L	124	7.2

547 **Table 3: The top mutations associated with phenotypic drug resistance**

548 Depicted is a survey of the resistance-associated mutations present in CRyPTIC isolates (7,25).
549 "VARIANT": non-synonymous amino acid mutations are denoted by upper case letters while
550 nucleotide substitutions for non-coding sequences are denoted by lower case letters. Negative
551 numbers denote substitutions in promoter regions; "GENE": genic region of interest in which
552 "Variant" can be found; "n": number of phenotypically resistant isolates with "VARIANT"; "%":
553 percentage of total phenotypically resistant isolates with "VARIANT".

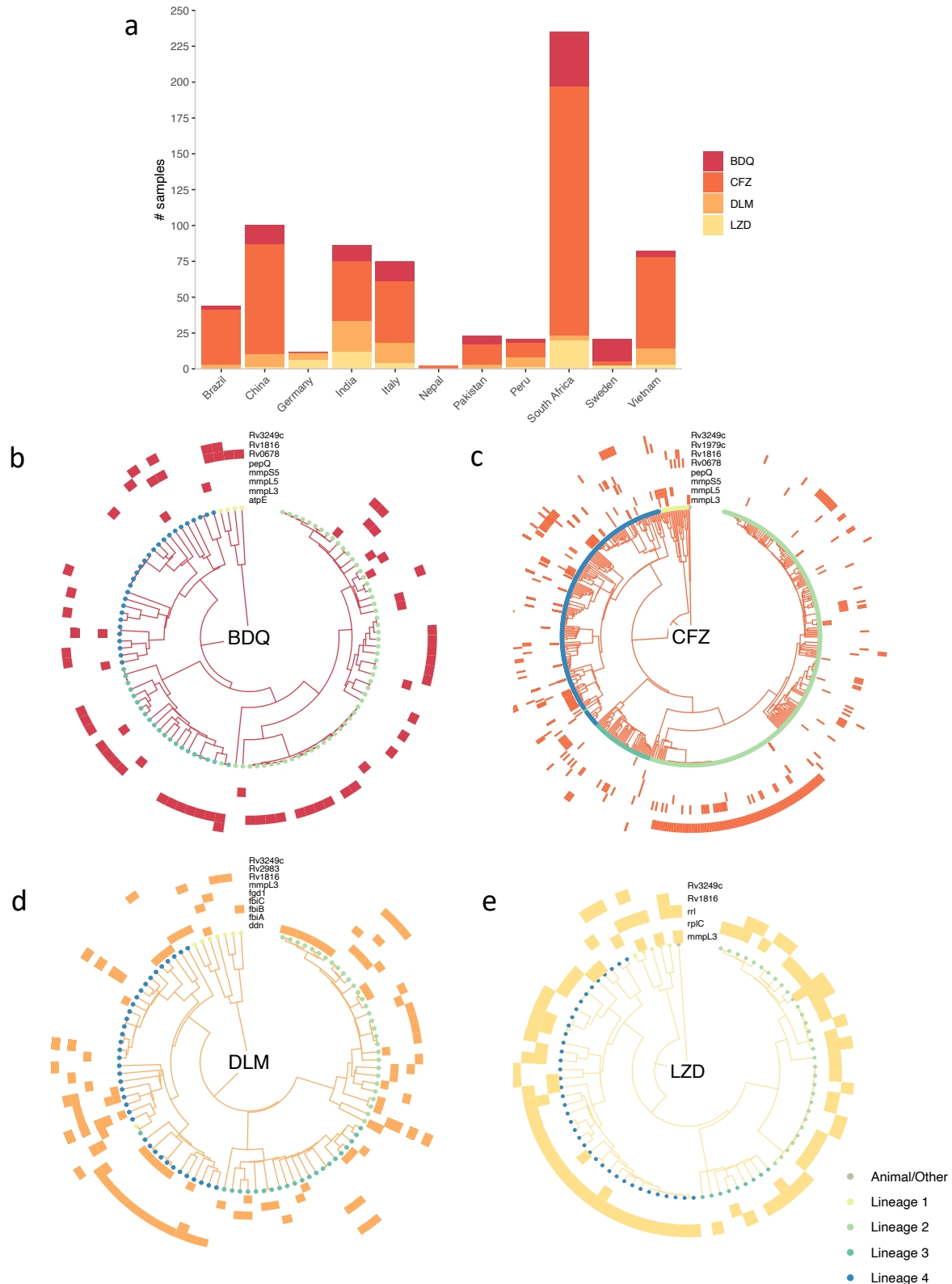
554

555

556 **Resistance to new and re-purposed drugs**

557 As previously stated, relatively few isolates are resistant to the NRDs,
558 bedaquiline ($n = 109$), clofazimine ($n = 525$), delamanid ($n = 186$) and linezolid ($n =$
559 156). South Africa contributed the greatest number of isolates resistant to bedaquiline,
560 clofazimine and linezolid (Fig. 5a), while China and India contributed the most isolates
561 resistant to delamanid. Since the collection protocol differed between laboratories it is
562 not possible to infer any differences in the relative prevalence of resistance to the
563 NRDs in these countries. The results of a survey of all non-synonymous mutations in
564 genes known or suspected to be involved in resistance to these four drugs (e.g.
565 *rv0678*, *mmpL5*, *pepQ*, *ddn*, *rplC*, *rrl* etc.) are depicted in Fig. 5b-e (38–42). Mutations
566 known to be associated with sensitivity were ignored, along with mutations that
567 occurred at a frequency of $\geq 5\%$ amongst all isolates (as 0.05% of total isolates are
568 resistant to the NRDs). In contrast to first- and second-line drugs, there are no
569 mutations within a single gene/small group of genes that can fully explain resistance
570 to any NRD, and indeed no single gene (if there were, they would be visible as
571 complete rings around the phylotrees in figure 5). Note that the role of most of these
572 mutations in resistance remains undetermined.

573



574

575 **Figure 5: Resistance to bedaquiline, clofazimine, delamanid and linezolid**
576 **amongst *M. tuberculosis* CRyPTIC isolates** a) The prevalence (within these data) of
577 resistance to bedaquiline (BDQ), clofazimine (CFZ), delamanid (DLM) and linezolid (LZD) per
578 country or origin or collection site. Phylogenrees are shown for isolates phenotypically resistant to b)
579 BDQ, c) CFZ, d) DLM and e) LZD. Tip point colours denote lineage. Each outer track represents

580 a gene thought to be associated with resistance and coloured blocks denote the presence of a
581 non-synonymous mutation in the relevant gene for a given isolate. Mutations in these genes that
582 are either associated with sensitivity or present in >5% of the collection of isolates as a whole were
583 ignored.

584

585

586 **Case study on rifampicin mono-resistance**

587 Around 1% of TB cases are rifampicin mono-resistant (RMR) and the frequency
588 is increasing (1,43). The WHO does not recommend isoniazid for RMR treatment,
589 despite it being effective; this is likely due to the reliance on assays such as Xpert®
590 MTB/RIF which cannot distinguish between RMR and MDR. Use of isoniazid could
591 improve treatment outcomes for RMR patients which are currently similar to that of
592 MDR TB, including a higher risk of death compared to drug susceptible infections
593 (44,45). Due to its low natural prevalence, RMR has been poorly studied to date but
594 increasingly large clinical TB datasets, such as the one presented here, make its study
595 now feasible.

596

597 For this case study, we defined RMR as any isolate that is rifampicin resistant
598 and isoniazid susceptible, and discounted isolates with no definite phenotype for either
599 drug. Of the 4,655 rifampicin resistant isolates in the compendium that also had a
600 phenotype for isoniazid, 302 (6.5%) were RMR. These isolates were contributed by
601 12 different countries, and we found South African and Nigerian contributions had a
602 significantly higher proportion of RMR isolates than that of the total dataset at 17.5%
603 ($p < 0.00001$) and 27.3% ($p = 0.00534$) respectively (Fig. 6a) compared with 6.5% for
604 the total dataset. We note that these proportions are influenced by sampling strategies
605 but the higher contribution of RMR isolates from South Africa is consistent with
606 previous studies (43).

607

608

609 ***Rifampicin mono-resistance is incorrectly predicted by current diagnostics***

610 A widely used, WHO-endorsed diagnostic tool, the Xpert® MTB/RIF assay,
611 uses a proxy whereby *any* SNP detected in the “rifampicin-resistance determining
612 region” (RRDR) of *rpoB* results in a prediction of MDR. However, the suitability of the
613 proxy is dependent upon prevalence of RMR in the population (43). We tested the
614 reliability of this on the 4,655 rifampicin resistant isolates in our dataset that had a
615 phenotype for isoniazid (Fig. 6b).

616

617 Of these isolates, 4,353 (93.5%) were MDR and 302 (6.5%) were RMR. 187 of
618 the MDR isolates had no RRDR mutation and therefore 4.0% of isolates in this study
619 would be predicted as false negative MDR by the Xpert® MTB/RIF assay. 276 of the
620 RMR isolates had a mutation in the RRDR of *rpoB* and so the Xpert® MTB/RIF assay
621 proxy would incorrectly predict 5.9% of the rifampicin resistant isolates as false
622 positive MDR cases. However, overall, the Xpert® MTB/RIF assay proxy correctly
623 predicts 89.5% of the rifampicin resistant isolates as MDR and 0.6% of the isolates as
624 non-MDR in this dataset, which suggests it is a reasonably successful diagnostic tool
625 with > 90% accuracy for MDR classification of rifampicin resistant isolates. As our
626 dataset is oversampled for resistance, it likely contains a higher prevalence of RMR
627 than the global average and hence the Xpert® MTB/RIF assay is likely to perform
628 better on more representative data. However, the analysis shows how the increasing
629 global levels of RMR TB cases could increase the number of false positive MDR
630 diagnoses by the Xpert® MTB/RIF assay, denying isoniazid treatment to a greater
631 number of patients who would then be moved on to less effective drugs.

632

633 ***There are genetic differences between rifampicin mono-resistant and***
634 ***multidrug resistant isolates***

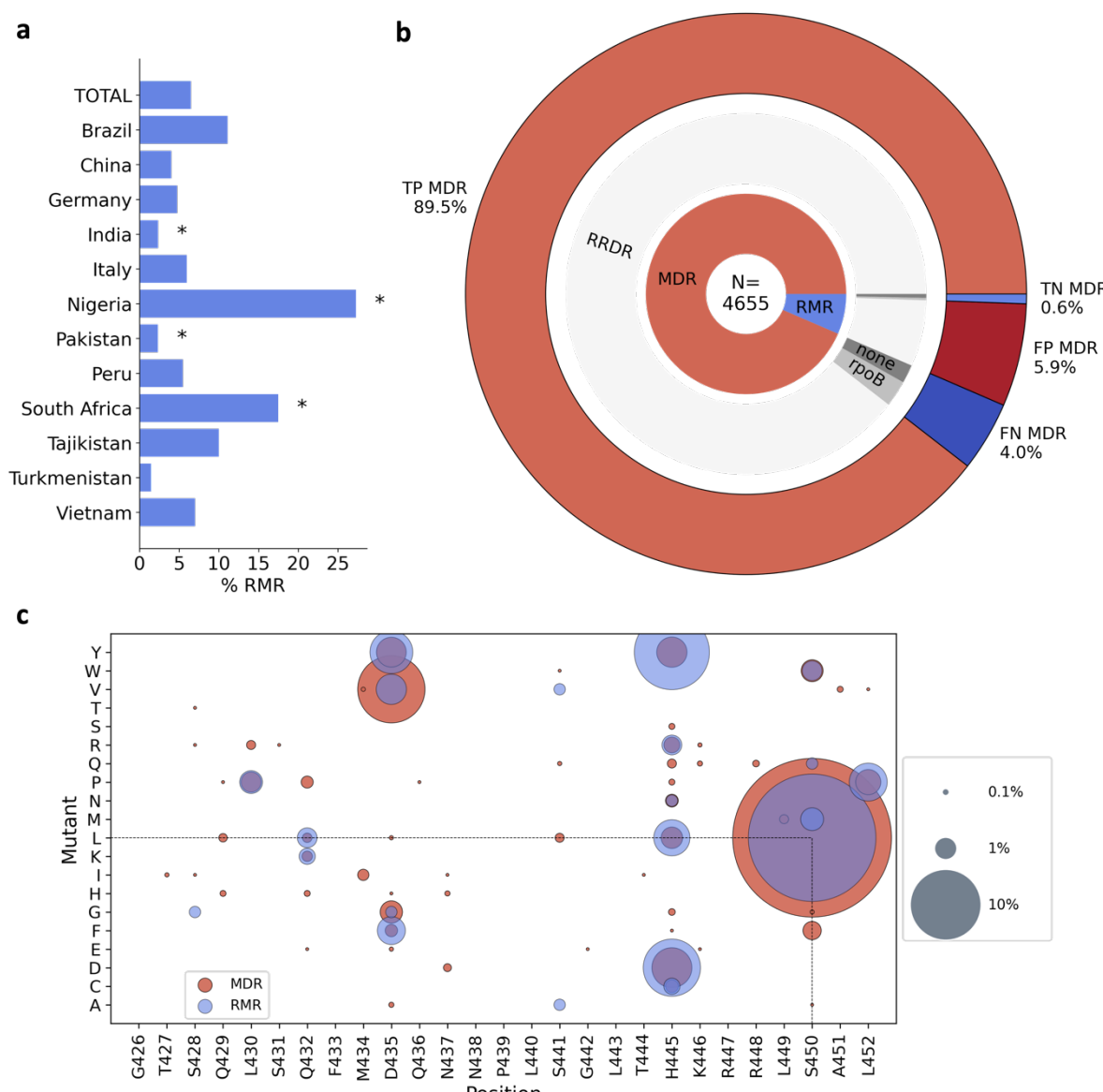
635 We have analysed our matched phenotypic and genotypic data to examine
636 whether there were any differences in the genetic determinants of rifampicin
637 resistance between RMR and MDR isolates as was seen in a recent study of South
638 African isolates (46). The proportion of RMR isolates with no *rpoB* mutation (5.3%, Fig.
639 6b) was significantly higher than that of MDR isolates (1.8%, $p < 0.00001$). This
640 suggests that non-target-mediated resistance mechanisms, such as upregulation of
641 rifampicin specific efflux pumps, could be more influential in providing protection
642 against rifampicin in RMR isolates than in MDR isolates.

643

644 The majority of RMR and MDR isolates contained one or more SNPs in *rpoB*,
645 with the most having at least one mutation in the RRDR. To date, several non-
646 synonymous RRDR mutations have been found in RMR *M. tuberculosis* isolates,
647 including the resistance conferring mutations S450L, H445D and D435Y, which are
648 also seen in MDR isolates (47,48). For both RMR and MDR isolates in this dataset,
649 the most common *rpoB* RRDR mutation seen was S450L (63.6% and 41.1% of
650 isolates respectively, Fig. 6c). Five mutations were present in RMR isolates that were
651 not seen in MDR isolates: S428G, S441A, S441V, S450M and S450Q, however these
652 were seen at low prevalence (< 2%) of RMR isolates. We found more RMR isolates
653 had His445 mutated than MDR isolates (27.8% of RMR and 9.5% of MDR, $p < 0.00001$), and mutations at Ser450 and Asp435 were more prevalent in MDR isolates
654 than RMR isolates (43.7% of RMR and 65.8% of MDR ($p < 0.00001$), and 9.3% of RMR
655 and 15.5% of MDR ($p = 0.00328$) respectively).

657

658 In RMR isolates we observed 27 different *rpoB* mutations that fall outside the
659 RRDR; 11 were found in RMR but not MDR isolates and all were seen at < 2%
660 prevalence (Fig. S6). The most common non-RRDR mutation in both MDR and RMR
661 isolates was a cytosine to thymine mutation 61 bases upstream of the *rpoB* start codon
662 (10.1% and 8.6% of isolates respectively). The resistance conferring mutations, *rpoB*
663 I491F, V695L and V170F, were seen at low proportions (< 2% of isolates) with no
664 significant difference between MDR and RMR isolates.



665
666
667 **Figure 6: Rifampicin mono resistance** a) Percentage of rifampicin resistant isolates that
668 are rifampicin mono-resistant (RMR) by country of isolate origin. * indicates RMR proportions that

669 were significantly different from that of the total dataset using a two tailed z-test with 95%
670 confidence. **b)** MDR predictions for rifampicin resistant isolates made using the Xpert® MTB/RIF
671 assay proxy. N is the total number of rifampicin resistant isolates. The inner ring shows the
672 proportion of rifampicin resistant isolates that are MDR and RMR. The middle ring represents the
673 proportions of MDR and RMR isolates that have a SNP (synonymous or non-synonymous) in the
674 RRDR of *rpoB* (RRDR), no RRDR SNP but a SNP elsewhere in the *rpoB* gene (*rpoB*) and no *rpoB*
675 mutations (none). The outer ring shows the expected true positive (TP), true negative (TN), false
676 positive (FP) and false negative (FN) MDR predictions of Xpert® MTB/RIF assay, based on the
677 SNPs present in the rifampicin resistant isolates. **c)** Non-synonymous mutations found in the
678 RRDR of *rpoB* in RMR isolates and MDR isolates. Presence of a coloured spot indicates that the
679 mutation was found in RMR/MDR isolates and spot size corresponds to the proportion of RMR or
680 MDR isolates carrying that mutation.

681
682
683
684

685 **Discussion**

686 This compendium of *M. tuberculosis* clinical isolates is the result of an extensive
687 global effort by the CRyPTIC consortium to better map the genetic variation associated
688 with drug resistance. Through its sheer size and by oversampling for resistance, the
689 compendium gives an unparalleled view of resistance and resistance patterns
690 amongst the panel of 13 antitubercular compounds studied. This study serves to
691 summarise the data within the compendium and to highlight the existence of the open-
692 access resource to the wider community to help better inform future treatment
693 guidelines and steer the development of improved diagnostics.

694
695

696 Starting with first-line drugs, molecular based diagnostic assays have vastly
697 improved the detection of and the speed at which we find drug resistant TB cases,
698 resulting in improved quality of care for patients. However, relying solely on these
699 diagnostic methods has several drawbacks. Aside from the Xpert® MTB/RIF assay
700 potentially increasing false positive MDR diagnoses as discussed earlier in the RMR

701 case study, the assay assumes isoniazid resistance upon detection of rifampicin
702 resistance. Thus, less is known about the prevalence of mono isoniazid resistance or
703 'true' cases of MDR (confirmed rifampicin *and* isoniazid resistance) (1) and with large
704 datasets such as this compendium, we can further investigate these important and
705 rarer clinical phenotypes (like that of RMR in our case study). Another example of a
706 rarer phenotype is that of isoniazid-resistant and rifampicin-susceptible (Hr-TB)
707 isolates; a greater number of these were contributed by CRyPTIC countries than RMR
708 isolates ($n = 1470$ versus $n = 302$), a pattern also recently observed in a global
709 prevalence study (49). A modified 6-month treatment regimen is now recommended
710 for Hr-TB (rifampicin, ethambutol, levofloxacin and pyrazinamide), and as a result of
711 inadequate diagnosis many of the 1.4 million global Hr-TB estimated cases would
712 have received inadequate and unnecessarily longer treatment regimens (1,42).
713 Encouragingly, CRyPTIC isolates with a Hr-TB background exhibited relatively low
714 levels of resistance to other antitubercular drugs, including those in the augmented
715 regimen (Fig. 4c). However, without appropriate tools to assess and survey this, we
716 will continue to misdiagnose and infectively treat these clinical cases. In 2018,
717 CRyPTIC and the 100,000 Genomes project demonstrated that genotypic prediction
718 from WGS correlates well with culture-based phenotype for first-line drugs, which is
719 reflected in our summary of the genetic catalogue applied to this dataset (Table 3) (7).
720 While predictions can be made to a high level of sensitivity and specificity, there is still
721 more to learn, as exemplified by the isolates in the compendium that despite being
722 resistant to rifampicin and isoniazid could not be described genetically (Table 2). This
723 shortfall, along with the limitations of molecular based diagnostic assays, highlights
724 the need for continual genetic surveillance and shines a favourable light on a WGS-
725 led approach.

726

727

728 A strength of this compendium lies with the data collated for second-line drugs.
729 A greater proportion of drug resistant isolates had additional resistance to
730 fluoroquinolones than second line injectable drugs (Fig. 4a). This could be due to more
731 widespread use of fluoroquinolones as well as their ease of administration and hence
732 them being recommended over injectables for longer MDR treatment regimens (1).
733 Concerningly, we found that resistance to levofloxacin and moxifloxacin, and
734 kanamycin and amikacin, were more common than resistance to the mycobacterial
735 specific drug ethambutol in an isoniazid and rifampicin susceptible background (Fig.
736 4b), suggesting a level of pre-existing resistance to second-line drugs. This concurs
737 with a systematic review that found patients previously prescribed fluoroquinolones
738 were three times more likely to have fluoroquinolone resistant TB (50). Careful
739 stewardship of fluoroquinolones, both in TB and other infectious diseases, will be
740 paramount for the success of treatment regimens. Despite variability in sample
741 collection, we observed high proportions of fluoroquinolone resistant MDR/RR isolates
742 from some countries and therefore suggest that MDR treatment regimens could be
743 improved by optimisation on a geographic basis.

744

745 Further treatment improvement could also be made by the selection of
746 appropriate drugs from each class. For example, the WHO recommends switching
747 from kanamycin to amikacin when treating MDR TB patients (51) and the compendium
748 supports this recommendation as we saw more resistance to kanamycin than amikacin
749 in all phenotypic backgrounds. For fluoroquinolones, more isolates were resistant to
750 levofloxacin than moxifloxacin in all phenotypic backgrounds suggesting moxifloxacin

751 may be the most appropriate fluoroquinolone to recommend, although we note this
752 conclusion is critically dependent on the validity of the cutoff, here an ECOFF, used to
753 infer resistance. However, the amenability of drugs to catalogue-based genetic
754 diagnostics is also an important consideration, and our data suggest levofloxacin
755 resistance could be predicted more reliably than moxifloxacin, with fewer false
756 positives predicted (Table 2). Testing for fluoroquinolone resistance using molecular
757 diagnostic tests remains limited. Global data from the past 15 years suggests that the
758 proportion of MDR/RR TB cases resistant to fluoroquinolones sits at around 20%, with
759 these cases primarily found in regions of high MDR-TB burden (1). While recently
760 approved tools, such as the Cepheid Xpert® MTB/XDR cartridge, will permit both
761 isoniazid and fluoroquinolone testing to be increased, the same pitfalls are to be
762 encountered regarding targeted diagnostic assays (52). In contrast, the genetic survey
763 in this study demonstrates the potential of WGS for genetic prediction of resistance to
764 second-line drugs and studies within the consortium to investigate this are underway.

765

766 The CRyPTIC compendium has facilitated the first global survey of resistance
767 to NRDs. Reassuringly, prevalence of resistance to the NRDs was substantially lower
768 than for first- and second-line agents in the dataset (Fig. 3a), and resistance to the
769 new drugs bedaquiline and delamanid was less common than the repurposed drugs
770 clofazimine and linezolid in an MDR/RR background (Fig. 4c). However, the presence
771 of higher levels of delamanid and clofazimine resistance than ethambutol resistance
772 in the isoniazid and rifampicin susceptible background does suggest some pre-existing
773 propensity towards NRD resistance (Fig. 4b).

774

775 Co-resistance between NRDs was seen in isolates in the compendium, the
776 most common being isolates resistant to both bedaquiline and clofazimine. This link is
777 well documented and has been attributed to shared resistance mechanisms such as
778 non-synonymous mutations in *Rv0678* which were found in both clofazimine and
779 bedaquiline resistant isolates in the compendium (42) (Fig. 5b,c). Increased
780 clofazimine use could further increase the prevalence of *M. tuberculosis* isolates with
781 clofazimine and bedaquiline co-resistance, limiting MDR treatment options including
782 using bedaquiline as the backbone of a shorter MDR regimen (53). Therefore,
783 proposed usage of clofazimine for other infectious diseases should be carefully
784 considered.

785

786 The WHO recommends against the use of bedaquiline and delamanid in
787 combination to prevent the development of co-resistance, which could occur relatively
788 quickly (54); the rate of spontaneous evolution of delamanid resistance *in vitro* has
789 been shown to be comparable to that of isoniazid, and likewise bedaquiline resistance
790 arises at a comparable rate to rifampicin resistance (55). In this compendium, 12.9%
791 of bedaquiline resistant isolates were resistant to delamanid and 7.1% of delamanid
792 resistant isolates were resistant to bedaquiline. Several scenarios could account for
793 this, including the presence of shared resistance mechanisms. For example, as
794 bedaquiline targets energy metabolism within the cell, changes to cope with
795 energy/nutrient imbalances upon the acquisition of resistance-associated ATPase
796 pump mutations may result in cross resistance to delamanid in a yet unknown or
797 unexplored mechanism (12). It is imperative that genetic determinants of resistance
798 are fully explored for the NRDs, as these are our current treatments of last resort, with
799 special attention given to those mechanisms that could be shared with other agents.

800 In the meantime, careful stewardship and phenotypic and genotypic surveillance of
801 the NRDs should be implemented, including linezolid and clofazimine which are now
802 group A and B drugs respectively for MDR treatment (1).

803

804 Several research avenues are being actively explored by the CRyPTIC
805 consortium that make further use of this compendium, including: *i*) relating genetic
806 mutations to quantitative changes in the minimum inhibitory concentrations of different
807 drugs (12); *ii*) genome-wide association studies (14); *iii*) training machine learning
808 models that can predict resistance (13); *iv*) exploration of the genetic determinants of
809 resistance to second line and NRDs (15). Collectively these studies share the same
810 aim of facilitating the implementation of WGS-directed resistance prediction in the
811 clinic. Finally, we urge other researchers to explore and analyse this large dataset of
812 *M. tuberculosis* clinical isolates and hope it will lead to a wave of new and inciteful
813 studies that will positively serve the TB community for years to come.

814

815

816 CRyPTIC Consortium Members

817 Alice Brankins^{5,*,**} and Kerri M Malone^{23,*,**}, Ivan Barilar¹, Simone Battaglia², Emanuele
818 Borroni², Angela Pires Branda^{3,4}, Andrea Maurizio Cabibbe², Joshua Carter⁶, Darren Chetty⁷,
819 Daniela Maria Cirillo², Pauline Claxton⁸, David A Cliftons⁵, Ted Cohen⁹, Jorge Coronel¹⁰, Derrick
820 W Crook⁵, Viola Dreyer¹, Sarah G Earles⁵, Vincent Escuyer¹¹, Lucilaine Ferrazoli⁴, George Fu
821 Gao¹², Jennifer Gardy¹³, Saheer Gharbia¹⁴, Kelen Teixeira Ghisi⁴, Arash Ghodousi^{2,15}, Ana Lúiza
822 Gibertoni Cruz⁵, Louis Grandjean¹⁶, Clara Grazian¹⁷, Ramona Groenheit¹⁸, Jennifer L
823 Guthrie^{19,20}, Wencong He¹², Harald Hoffmann^{21,22}, Sarah J Hoosdally⁵, Martin Hunt^{23,5}, Nazir
824 Ahmed Ismail²⁴, Lisa Jarrett²⁵, Lavanja Joseph²⁴, Ruwen Jou²⁶, Priti Kamblu²⁷, Rukhsar Khot²⁷,
825 Jeff Knaggs^{23,5}, Anastasia Koch²⁸, Donna Kohlerschmidt¹¹, Samaneh Kouchaki^{5,29}, Alexander S
826 Lachapelles, Ajit Lalvani³⁰, Simon Grandjean Lapierre³¹, Ian F Laurenson⁸, Brice Letcher²³,
827 Wan-Hsuan Lin²⁶, Chunfa Liu¹², Dongxin Liu¹², Ayan Mandal³², Mikael Mansjo¹⁸, Daniela
828 Matias²⁵, Graeme Meintjes²⁸, Flávia de Freitas Mendes⁴, Matthias Merker¹, Marina Mihalic²²,

829 James Millard⁷, Paolo Miotto², Nerges Mistry³², David Moore^{33,10}, Kimberlee A Musser¹¹,
830 Dumisani Ngcamu²⁴, Hoang Ngoc Nhung³⁴, Stefan Niemann^{1,35}, Kayzad Soli Nilgiriwala³²,
831 Camus Nimmo¹⁶, Max O'Donnell³⁶, Nana Okozi²⁴, Rosangela Siqueira Oliveira⁴, Shaheed Vally
832 Omar²⁴, Nicholas Paton³⁷, Timothy EA Peto⁵, Juliana Maira Watanabe Pinhata⁴, Sara Plesnik²²,
833 Zully M Puyen³⁸, Marie Sylvianne Rabodoarivel³⁹, Niaina Rakotosamimanana³⁹, Paola MV
834 Rancoita¹⁵, Priti Rathod²⁵, Esther Robinson²⁵, Gillian Rodgers⁵, Camilla Rodrigues²⁷, Timothy C
835 Rodwell^{40,41}, Aysha Roohi⁵, David Santos-Lazaro³⁸, Sanchi Shah³², Thomas Andreas Kohl¹,
836 Grace Smith^{25,14}, Walter Solano¹⁰, Andrea Spitaleri^{2,15}, Philip Supply⁴², Adrie JC Steyn⁷,
837 Utkarsha Surve²⁷, Sabira Tahseen⁴³, Nguyen Thuy Thuong Thuong³⁴, Guy Thwaites^{34,5},
838 Katharina Todt²², Alberto Trovato², Christian Utpatel¹, Annelies Van Rie⁴⁴, Srinivasan Vijay⁴⁵,
839 Timothy M Walker^{5,34}, A Sarah Walkers⁵, Robin Warren⁴⁶, Jim Werngren¹⁸, Maria Wijkander¹⁸,
840 Robert J Wilkinson^{47,48,30}, Daniel J Wilson⁵, Penelope Wintringer²³, Yu-Xin Xiao²⁶, Yang Yang⁵,
841 Zhao Yanlin¹², Shen-Yuan Yao²⁴, Baoli Zhu⁴⁹, Philip W Fowlers⁵, Zamin Iqbal²³**

842

843 *equal contribution authors

844 **co-corresponding authors

845 **Institutions**

846 ¹Research Center Borstel, Borstel, Germany

847 ²IRCCS San Raffaele Scientific Institute, Milan, Italy

848 ³Oswaldo Cruz Foundation, Rio de Janeiro, Brazil

849 ⁴Institute Adolfo Lutz, São Paulo, Brazil

850 ⁵University of Oxford, Oxford, UK

851 ⁶Stanford University School of Medicine, Stanford, USA

852 ⁷Africa Health Research Institute, Durban, South Africa

853 ⁸Scottish Mycobacteria Reference Laboratory, Edinburgh, UK

854 ⁹Yale School of Public Health, Yale, USA

855 ¹⁰Universidad Peruana Cayetano Heredia, Lima, Perú

856 ¹¹Wadsworth Center, New York State Department of Health, Albany, USA

857 ¹²Chinese Center for Disease Control and Prevention, Beijing, China

858 ¹³Bill & Melinda Gates Foundation, Seattle, USA

859 ¹⁴UK Health Security Agency, London, UK

860 ¹⁵Vita-Salute San Raffaele University, Milan, Italy

861 ¹⁶University College London, London, UK

862 ¹⁷University of New South Wales, Sydney, Australia

863 ¹⁸Public Health Agency of Sweden, Solna, Sweden

864 ¹⁹The University of British Columbia, Vancouver, Canada

865 20Public Health Ontario, Toronto, Canada
866 21SYNLAB Gauting, Munich, Germany
867 22Institute of Microbiology and Laboratory Medicine, IMLred, WHO-SRL Gauting, Germany
868 23EMBL-EBI, Hinxton, UK
869 24National Institute for Communicable Diseases, Johannesburg, South Africa

870 25UK Health Security Agency, Birmingham, UK
871 26Taiwan Centers for Disease Control, Taipei, Taiwan
872 27Hinduja Hospital, Mumbai, India
873 28University of Cape Town, Cape Town, South Africa
874 29University of Surrey, Guildford, UK
875 30Imperial College, London, UK
876 31Université de Montréal, Canada
877 32The Foundation for Medical Research, Mumbai, India
878 33London School of Hygiene and Tropical Medicine, London, UK
879 34Oxford University Clinical Research Unit, Ho Chi Minh City, Viet Nam
880 35German Center for Infection Research (DZIF), Hamburg-Lübeck-Borstel-Riems, Germany
881 36Colombia University Irving Medical Center, New York, USA
882 37National University of Singapore, Singapore
883 38Instituto Nacional de Salud, Lima, Perú
884 39Institut Pasteur de Madagascar, Antananarivo, Madagascar
885 40FIND, Geneva, Switzerland
886 41University of California, San Diego, USA
887 42Univ. Lille, CNRS, Inserm, CHU Lille, Institut Pasteur de Lille, U1019 - UMR 9017 - CIIL -
888 Center for Infection and Immunity of Lille, F-59000 Lille, France
889 43National TB Reference Laboratory, National TB Control Program, Islamabad, Pakistan
890 44University of Antwerp, Antwerp, Belgium
891 45University of Edinburgh, Edinburgh, UK
892 46Stellenbosch University, Cape Town, South Africa
893 47Wellcome Centre for Infectious Diseases Research in Africa, Cape Town, South Africa
894 48Francis Crick Institute, London, UK
895 49Institute of Microbiology, Chinese Academy of Sciences, Beijing, China

896

897

898 **Author contributions**

899 D.W.C, T.E.A.P, S.H, A.L.G.C, A.W.S, T.M.W, P.W.F, D.M.C designed the CRyPTIC
900 study and all contributing laboratories collected samples and provided data. MIC data

901 and genetic information was retrieved and processed by P.W.F, S.H, A.L.G.C, Z.I, M.H
902 and J.K. A.B and K.M.M designed and performed all analyses for this manuscript. A.B
903 and K.M.M wrote the manuscript with feedback from CRyPTIC partners.

904

905
906 **Acknowledgements**

907 We thank Faisal Masood Khanzada and Alamdar Hussain Rizvi (NTRL, Islamabad,
908 Pakistan), Angela Starks and James Posey (Centers for Disease Control and
909 Prevention, Atlanta, USA), and Juan Carlos Toro and Solomon Ghebremichael (Public
910 Health Agency of Sweden, Solna, Sweden), Iñaki Comas and Álvaro Chiner-Oms
911 (Instituto de Biología Integrativa de Sistemas, Valencia, Spain; CIBER en
912 Epidemiología y Salud Pública, Valencia, Spain; Instituto de Biomedicina de Valencia,
913 IBV-CSIC, Valencia, Spain).

914

915 **Funding bodies**

916 This work was supported by Wellcome Trust/Newton Fund-MRC Collaborative Award
917 (200205/Z/15/Z); and Bill & Melinda Gates Foundation Trust (OPP1133541). Oxford
918 CRyPTIC consortium members are funded/supported by the National Institute for
919 Health Research (NIHR) Oxford Biomedical Research Centre (BRC), the views
920 expressed are those of the authors and not necessarily those of the NHS, the NIHR
921 or the Department of Health, and the National Institute for Health Research (NIHR)
922 Health Protection Research Unit in Healthcare Associated Infections and Antimicrobial
923 Resistance, a partnership between Public Health England and the University of
924 Oxford, the views expressed are those of the authors and not necessarily those of the
925 NIHR, Public Health England or the Department of Health and Social Care. J.M. is
926 supported by the Wellcome Trust (203919/Z/16/Z). Z.Y. is supported by the National

927 Science and Technology Major Project, China Grant No. 2018ZX10103001. K.M.M. is
928 supported by EMBL's EIPOD3 programme funded by the European Union's Horizon
929 2020 research and innovation programme under Marie Skłodowska Curie Actions.
930 T.C.R. is funded in part by funding from Unitaid Grant No. 2019-32-FIND MDR. R.S.O.
931 is supported by FAPESP Grant No. 17/16082-7. L.F. received financial support from
932 FAPESP Grant No. 2012/51756-5. B.Z. is supported by the National Natural Science
933 Foundation of China (81991534) and the Beijing Municipal Science & Technology
934 Commission (Z201100005520041). N.T.T.T. is supported by the Wellcome Trust
935 International Intermediate Fellowship (206724/Z/17/Z). G.T. is funded by the
936 Wellcome Trust. R.W. is supported by the South African Medical Research Council.
937 J.C. is supported by the Rhodes Trust and Stanford Medical Scientist Training
938 Program (T32 GM007365). A.L. is supported by the National Institute for Health
939 Research (NIHR) Health Protection Research Unit in Respiratory Infections at Imperial
940 College London. S.G.L. is supported by the Fonds de Recherche en Santé du Québec.
941 C.N. is funded by Wellcome Trust Grant No. 203583/Z/16/Z. A.V.R. is supported by
942 Research Foundation Flanders (FWO) under Grant No. G0F8316N (FWO Odysseus).
943 G.M. was supported by the Wellcome Trust (098316, 214321/Z/18/Z, and
944 203135/Z/16/Z), and the South African Research Chairs Initiative of the Department
945 of Science and Technology and National Research Foundation (NRF) of South Africa
946 (Grant No. 64787). The funders had no role in the study design, data collection, data
947 analysis, data interpretation, or writing of this report. The opinions, findings and
948 conclusions expressed in this manuscript reflect those of the authors alone. L.G. was
949 supported by the Wellcome Trust (201470/Z/16/Z), the National Institute of Allergy and
950 Infectious Diseases of the National Institutes of Health under award number
951 1R01AI146338, the GOSH Charity (VC0921) and the GOSH/ICH Biomedical

952 Research Centre (www.nihr.ac.uk). A.B. is funded by the NDM Prize Studentship from
953 the Oxford Medical Research Council Doctoral Training Partnership and the Nuffield
954 Department of Clinical Medicine. D.J.W. is supported by a Sir Henry Dale Fellowship
955 jointly funded by the Wellcome Trust and the Royal Society (Grant No. 101237/Z/13/B)
956 and by the Robertson Foundation. A.S.W. is an NIHR Senior Investigator. T.M.W. is a
957 Wellcome Trust Clinical Career Development Fellow (214560/Z/18/Z). A.S.L. is
958 supported by the Rhodes Trust. R.J.W. receives funding from the Francis Crick
959 Institute which is supported by Wellcome Trust, (FC0010218), UKRI (FC0010218),
960 and CRUK (FC0010218). T.C. has received grant funding and salary support from US
961 NIH, CDC, USAID and Bill and Melinda Gates Foundation. The computational aspects
962 of this research were supported by the Wellcome Trust Core Award Grant Number
963 203141/Z/16/Z and the NIHR Oxford BRC. Parts of the work were funded by the
964 German Center of Infection Research (DZIF). The Scottish Mycobacteria Reference
965 Laboratory is funded through National Services Scotland. The Wadsworth Center
966 contributions were supported in part by Cooperative Agreement No. U60OE000103
967 funded by the Centers for Disease Control and Prevention through the Association of
968 Public Health Laboratories and NIH/NIAID grant AI-117312. Additional support for
969 sequencing and analysis was contributed by the Wadsworth Center Applied Genomic
970 Technologies Core Facility and the Wadsworth Center Bioinformatics Core. SYNLAB
971 Holding Germany GmbH for its direct and indirect support of research activities in the
972 Institute of Microbiology and Laboratory Medicine Gauting. N.R. thanks the
973 Programme National de Lutte contre la Tuberculose de Madagascar.
974
975
976

977 **Wellcome Trust Open Access**

978 This research was funded in part, by the Wellcome Trust/Newton Fund-MRC
979 Collaborative Award [200205/Z/15/Z]. For the purpose of Open Access, the author has
980 applied a CC BY public copyright licence to any Author Accepted Manuscript version
981 arising from this submission.

982

983 This research was funded, in part, by the Wellcome Trust [214321/Z/18/Z, and
984 203135/Z/16/Z]. For the purpose of open access, the author has applied a CC BY
985 public copyright licence to any Author Accepted Manuscript version arising from this
986 submission.

987

988

989 **Competing Interest**

990

991 E.R. is employed by Public Health England and holds an honorary contract with
992 Imperial College London. I.F.L. is Director of the Scottish Mycobacteria Reference
993 Laboratory. S.N. receives funding from German Center for Infection Research,
994 Excellenz Cluster Precision Medicine in Chronic Inflammation, Leibniz Science
995 Campus Evolutionary Medicine of the LUNG (EvoLUNG)tion EXC 2167. P.S. is a
996 consultant at Genoscreen. T.R. is funded by NIH and DoD and receives salary support
997 from the non-profit organization FIND. T.R. is a co-founder, board member and
998 shareholder of Verus Diagnostics Inc, a company that was founded with the intent of
999 developing diagnostic assays. Verus Diagnostics was not involved in any way with
1000 data collection, analysis or publication of the results. T.R. has not received any
1001 financial support from Verus Diagnostics. UCSD Conflict of Interest office has
1002 reviewed and approved T.R.'s role in Verus Diagnostics Inc. T.R. is a co-inventor of a
1003 provisional patent for a TB diagnostic assay (provisional patent #: 63/048.989). T.R. is

1004 a co-inventor on a patent associated with the processing of TB sequencing data
1005 (European Patent Application No. 14840432.0 & USSN 14/912,918). T.R. has agreed
1006 to “donate all present and future interest in and rights to royalties from this patent” to
1007 UCSD to ensure that he does not receive any financial benefits from this patent. S.S.
1008 is working and holding ESOPs at HaystackAnalytics Pvt. Ltd. (Product: Using whole
1009 genome sequencing for drug susceptibility testing for *Mycobacterium tuberculosis*).
1010 G.F.G. is listed as an inventor on patent applications for RBD-dimer-based CoV
1011 vaccines. The patents for RBD-dimers as protein subunit vaccines for SARS-CoV-2
1012 have been licensed to Anhui Zhifei Longcom Biopharmaceutical Co. Ltd, China.

1013

1014

1015

1016 **Supplemental Information**

1017

1018 **S1. Lineages of the *M. tuberculosis* isolates of the compendium.**

1019

1020 Isolates of the ancient Indo-oceanic lineage/L1 ($n = 1,150$) were mostly
1021 contributed by India ($n = 676$ isolates) and Vietnam ($n = 283$ isolates). 85% of the L1
1022 Indian isolates belong to sub-lineages 1.1.2 and 1.2.2 while 66% of the Vietnamese
1023 isolates are sub-lineage 1.1.1.1. No L1 isolates were contributed by 10 of the 23
1024 countries in this study with only 2 isolates collected in South America (one in each of
1025 Brazil and Peru).

1026

1027 There are 5,598 L2 (East Asian) isolates, making it the second largest group in
1028 the dataset. L2 was found most prevalent in Asia and Europe with the largest

1029 proportion found in amongst isolates contributed by China ($n = 722$, 64% of isolates)
1030 and India ($n = 1,573$, 39% of isolates). Sub-lineages 2.2 and 2.2.7 dominate the L2
1031 isolates ($n = 1,421$ and 1,249 respectively); 2.2 was found mostly amongst Peruvian
1032 and South African isolates ($n = 231$ and 161 respectively) apart from those contributed
1033 by the Asian countries of Vietnam ($n = 271$), China ($n = 284$) and India ($n = 272$), while
1034 85% of sub-lineage 2.2.7 isolates were contributed by South Africa ($n = 206$), Vietnam
1035 ($n = 164$) and India ($n = 691$). 70% of sub-lineage 2.2.1 originated from South Africa
1036 (10% of isolates found here) and has recently been associated with more favourable
1037 transmission rates (56). Lastly, 86% and 72% of isolates contributed by Kyrgyzstan
1038 and Turkmenistan respectively belong to L2 with sub-lineage 2.2.10 dominating (16/24
1039 and 75/86 isolates for both countries respectively). 2.2.10 has been previously
1040 described as restricted to Central Asia and this is reflected in the compendium (57).

1041

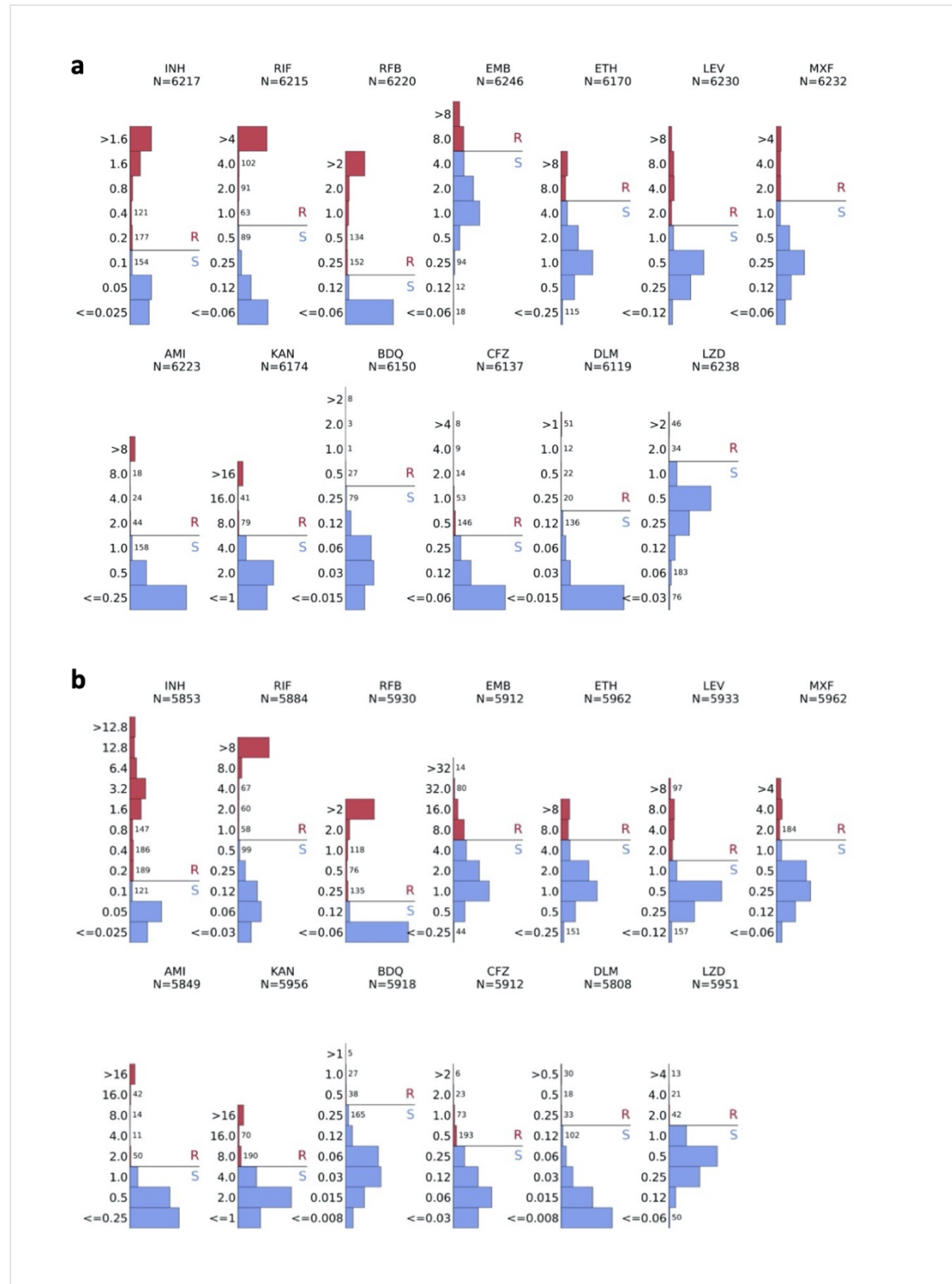
1042 The majority (1184/1850, 65%) of L3 (East African/Indian) isolates were
1043 contributed by India, followed by 19.6% (363/1850) isolates from Pakistan. L3 is
1044 typically under-sampled and under-studied in current databases and biobanks in
1045 comparison to L2 and L4; the L3 isolates in this study are the largest collected to date
1046 in a single study (31).

1047

1048 L4 (Euro-American) is the largest lineage group in the compendium ($n = 6,572$).
1049 Isolates donated from Peru dominate; 87% of all L4 isolates are Peruvian with 4.1.2.1
1050 and 4.3.3 being the most prevalent sub-lineages (24% and 22% respectively). There
1051 are 34 different L4 sub-lineages in the dataset, making L4 the most diverse in
1052 comparison to the other lineage groupings.

1053

1054 There were no L5 isolates found in the compendium and only 6 L6 isolates were
1055 identified. Animal-restricted pathogenic mycobacterial isolates are also rare in the
1056 compendium; only 16 cases were identified ($n = 15$ *M. bovis* and $n = 1$ *M. caprae*).
1057
1058



1059

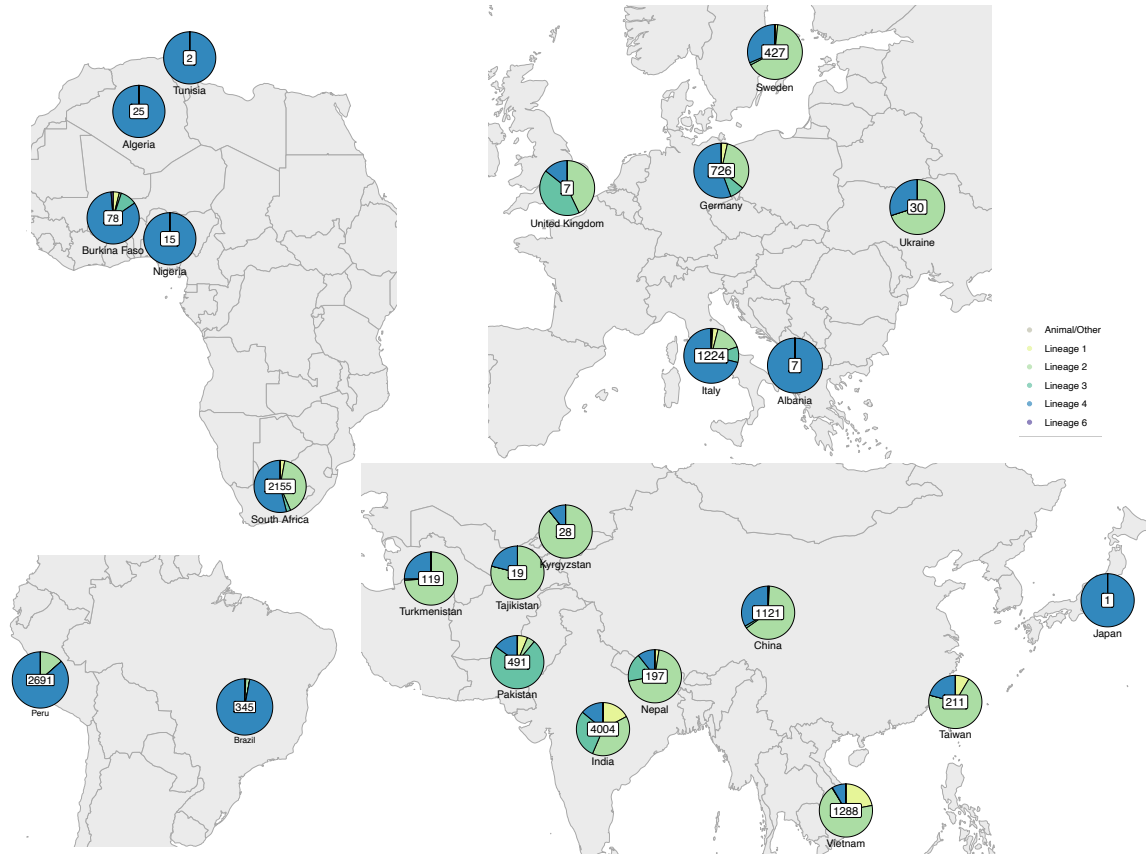
1060 **Figure S1: Per drug MIC distributions of isolates plated on CRyPTIC designed**
1061 **variations on the Thermo Fischer Sensititre MYCOTB MIC plate; UKMYC5 (a) and**
1062 **UKMYC6 (b).** The solid black line represents the epidemiological resistance cut-off (ECOFF) for
1063 each drug as determined by (11). Isolates with an MIC above the cut-off are considered resistant.
1064 N denotes the total number of isolates tested on each plate that returned a phenotype for each
1065 drug.

1066
1067
1068

DRUG	ECOFF
Isoniazid	0.1
Rifampicin	0.5
Rifabutin	0.12
Ethambutol	4
Ethionamide	4
Levofloxacin	1
Moxifloxacin	1
Amikacin	1
Kanamycin	4
Bedaquiline	0.25
Clofazimine	0.25
Delamanid	0.12
Linezolid	1

1069 **Table S1: Epidemiological cut-off values (ECOFFs) used to binarize MIC**
1070 **measurements into resistant and susceptible.** Isolates with an MIC above the cut-off
1071 are considered resistant and those at or below the cut-off as susceptible.

1072
1073



1074
1075
1076
1077
1078
1079
1080
1081

1082
1083
1084
1085
1086
1087
1088
1089

	Animal/ other	L1	L2	L3	L4	L6	Total
Albania	0	0	0	0	7	0	7
Algeria	0	0	0	0	25	0	25
Brazil	1	1	8	0	335	0	345
Burkina Faso	0	3	1	8	65	1	78
China	7	2	722	16	374	0	1121
Germany	1	25	235	61	403	1	726
India	11	676	1573	1184	560	0	4004
Italy	11	38	192	113	866	4	1224
Japan	0	0	0	0	1	0	1
Kyrgyzstan	0	0	25	0	3	0	28
Nepal	0	5	137	34	21	0	197
Nigeria	0	0	0	0	15	0	15
Pakistan	1	30	23	363	74	0	491
Peru	2	1	360	0	2328	0	2691
South Africa	1	61	874	57	1162	0	2155
Sweden	0	7	280	6	134	0	427
Taiwan	0	18	149	0	44	0	211
Tajikistan	0	0	15	0	4	0	19
Tunisia	0	0	0	0	2	0	2
Turkmenistan	0	0	88	1	30	0	119
Ukraine	0	0	21	0	9	0	30
UK	0	0	3	3	1	0	7
Vietnam	0	283	892	4	109	0	1288
Total	35	1150	5598	1850	6572	6	15211

1090 **Table S2: Lineages –v- geographical location of origin/contribution for CRyPTIC**
1091 **isolates**

1092

1093

1094

1095

1096

1097

1098

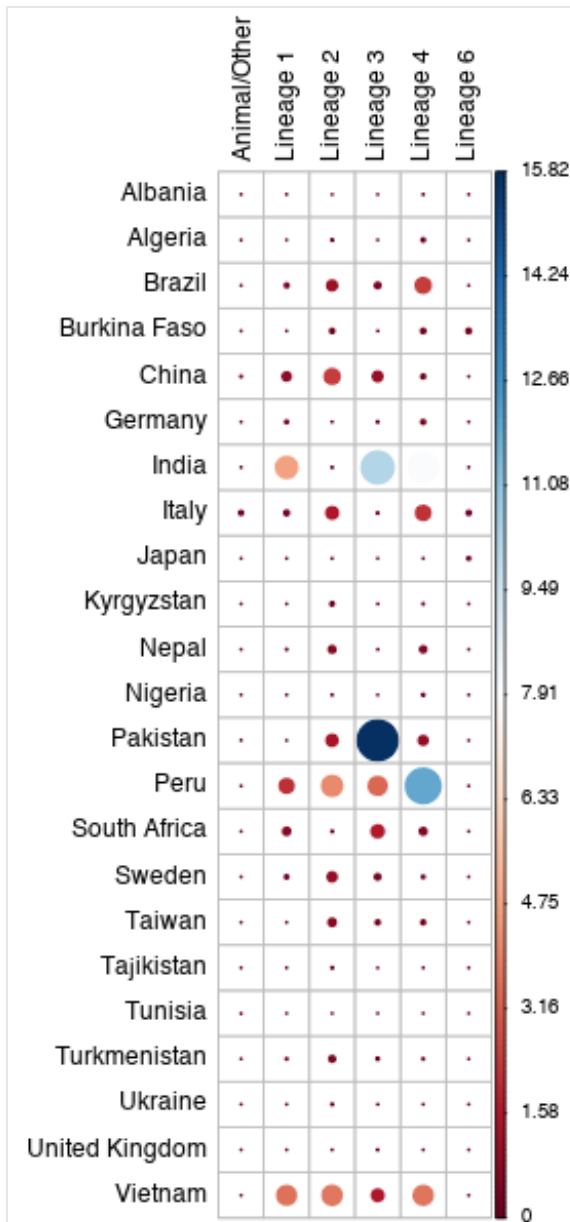
1099

	ALB	ALG	BRZ	BFA	CHN	GER	IND	ITL	JPN	KGZ	NPL	NGA	PAK	PER	ZAF	SWE	TWN	TJK	TUN	TKM	UKR	UK	VNM
1	0	0	0	0	0	0	1	0	0	0	0	0	0	0	0	0	0	0	0	0	0	0	0
1.1.1	0	0	0	2	0	0	1	2	0	0	0	0	0	0	0	0	0	0	0	0	0	0	38
1.1.1.1	0	0	0	0	0	2	0	0	0	0	0	0	0	0	0	0	0	0	0	0	0	0	188
1.1.2	0	0	0	1	1	12	316	16	0	0	2	0	23	0	0	1	0	6	0	0	0	0	0
1.1.3	0	0	1	0	0	1	52	4	0	0	1	0	1	0	6	0	0	0	0	0	0	0	2
1.2.1	0	0	0	0	0	8	12	11	0	0	0	0	0	1	0	3	16	0	0	0	0	0	24
1.2.2	0	0	0	0	1	2	259	5	0	0	2	0	4	0	54	3	1	0	0	0	0	0	1
2	0	0	0	0	0	1	0	0	0	0	0	0	0	0	0	0	0	0	0	0	0	0	0
2.1	0	0	0	0	1	1	0	0	0	0	0	0	0	1	0	0	20	0	0	0	0	0	34
2.2	0	0	5	1	284	19	272	14	0	0	68	0	6	231	181	13	56	0	0	0	0	0	271
2.2.1	0	0	0	0	37	4	2	2	0	0	0	0	0	3	224	1	21	0	0	0	0	0	26
2.2.10	0	0	0	0	1	117	1	84	0	16	0	0	3	0	0	70	0	5	0	75	9	1	0
2.2.2	0	0	0	0	32	8	5	11	0	1	0	0	1	0	0	1	5	0	0	0	1	0	8
2.2.3	0	0	2	0	172	3	290	4	0	0	21	0	2	1	3	1	10	0	0	0	0	0	100
2.2.4	0	0	0	0	3	3	4	8	0	0	0	0	0	0	37	1	1	0	0	0	0	0	70
2.2.5	0	0	0	0	59	1	12	5	0	0	0	0	2	84	1	1	13	0	0	0	0	0	45
2.2.6	0	0	1	0	22	8	226	2	0	0	9	0	7	4	204	1	4	0	0	0	0	0	154
2.2.7	0	0	0	0	97	4	691	5	0	1	38	0	0	20	206	5	18	0	0	0	0	0	164
2.2.8	0	0	0	0	4	0	42	0	0	0	1	0	2	0	0	0	0	0	0	0	0	0	2
2.2.9	0	0	0	0	0	64	0	51	0	6	0	0	0	2	0	174	0	10	0	11	11	2	0
3	0	0	0	8	15	37	828	81	0	0	28	0	346	0	34	5	0	0	0	1	0	2	2
3.1.1	0	0	0	0	0	17	17	25	0	0	1	0	0	0	19	1	0	0	0	0	0	1	2
3.1.2	0	0	0	0	1	5	201	3	0	0	1	0	7	0	2	0	0	0	0	0	0	0	0
3.1.2.1	0	0	0	0	0	2	119	3	0	0	4	0	6	0	0	0	0	0	0	0	0	0	0
4	0	0	1	0	6	4	0	6	0	0	0	0	0	100	1	1	0	0	0	1	0	0	0
4.1	0	0	0	1	0	1	0	2	0	0	0	0	0	0	0	0	0	0	0	0	0	0	0
4.1.1	0	0	0	0	0	6	5	10	0	0	1	0	0	154	13	1	0	0	0	0	0	0	0
4.1.1.1	0	0	5	0	1	3	20	5	0	0	1	0	2	5	54	1	0	0	0	0	0	0	1
4.1.1.2	0	0	0	0	0	0	4	1	0	0	0	0	0	0	6	0	0	0	0	0	0	0	0
4.1.1.3	0	0	1	6	1	0	30	7	1	0	3	0	2	68	138	0	0	0	0	0	0	0	1
4.1.2	0	0	13	0	0	15	3	26	0	1	0	0	0	31	43	0	0	0	0	0	0	0	10
4.1.2.1	1	8	87	10	0	111	56	183	0	0	3	2	4	653	54	5	0	1	0	0	1	0	17
4.1.3	0	0	0	5	0	0	0	6	0	0	0	1	0	0	0	0	0	0	0	0	0	0	0
4.10	4	6	35	5	1	110	166	207	0	1	3	0	28	128	170	4	5	2	1	6	2	0	12
4.2	0	0	0	0	3	1	0	1	0	0	0	0	0	0	0	0	0	0	0	0	0	0	0
4.2.1	0	0	0	0	0	9	3	46	0	0	1	0	2	0	2	4	0	0	0	8	3	1	0
4.2.2	0	1	0	0	53	31	76	51	0	0	5	0	12	2	10	10	1	0	0	0	0	0	11
4.2.2.1	0	0	0	0	0	5	0	9	0	0	0	0	0	0	0	0	0	0	0	0	0	0	0
4.3	0	0	17	0	0	0	0	1	0	0	0	0	0	96	1	0	0	0	0	0	0	0	0
4.3.1	0	3	0	1	0	1	2	21	0	0	0	0	0	8	0	1	0	0	0	0	0	0	1
4.3.2	0	1	10	0	0	3	1	8	0	0	0	0	0	245	21	0	0	0	0	0	0	0	0
4.3.2.1	0	0	0	0	0	0	0	0	0	0	0	0	0	0	234	0	0	0	0	0	0	0	0
4.3.3	1	4	34	2	0	33	99	81	0	1	1	0	0	576	120	102	2	1	1	11	2	0	1
4.3.4	0	0	1	0	0	0	8	0	0	0	0	0	0	1	0	0	0	0	0	0	0	0	0
4.3.4.1	0	0	70	0	0	2	6	3	0	0	0	0	0	60	22	2	1	0	0	0	0	0	0
4.3.4.2	0	0	38	0	0	6	7	27	0	0	0	0	0	132	12	0	0	0	0	0	0	1	0
4.3.4.2.1	0	0	0	0	0	2	1	1	0	0	0	0	0	0	75	0	0	0	0	0	0	0	0
4.4	0	0	0	0	0	0	13	0	0	0	0	0	0	1	0	0	0	0	0	0	0	0	0
4.4.1	0	0	10	0	0	0	0	2	0	0	0	0	0	11	0	0	0	0	0	0	0	0	0
4.4.1.1	0	0	4	0	0	16	4	66	0	0	1	0	0	22	180	2	0	0	0	0	0	0	4
4.4.1.2	0	0	0	0	0	1	25	3	0	0	0	0	0	2	0	0	0	0	0	0	0	0	3
4.4.2	0	0	0	0	124	1	4	1	0	0	0	0	0	4	0	0	5	0	0	0	0	0	16
4.5	0	0	0	0	179	28	15	14	0	0	1	0	18	5	1	0	30	0	0	3	0	0	29
4.6	0	1	0	1	0	1	1	7	0	0	0	2	0	0	0	0	0	0	0	0	0	0	0
4.6.1.1	0	0	0	0	0	1	0	0	0	0	0	0	0	0	0	0	0	0	0	0	0	0	0
4.6.1.2	0	0	0	0	0	1	0	0	0	0	0	0	0	0	0	1	0	0	0	0	0	0	0
4.6.2	0	0	0	0	0	2	2	14	0	0	0	0	4	0	0	0	0	0	0	0	0	0	0
4.6.2.1	0	0	0	0	0	0	1	0	0	0	1	0	1	0	0	0	0	0	0	0	0	0	0
4.6.2.2	1	0	0	0	34	0	8	1	55	0	0	0	10	1	0	1	0	0	0	0	0	0	3

1100 **Table S3: Sub-lineages –v– geographical location of origin/contribution for**
1101 **CRyPTIC isolates**

1102

1103

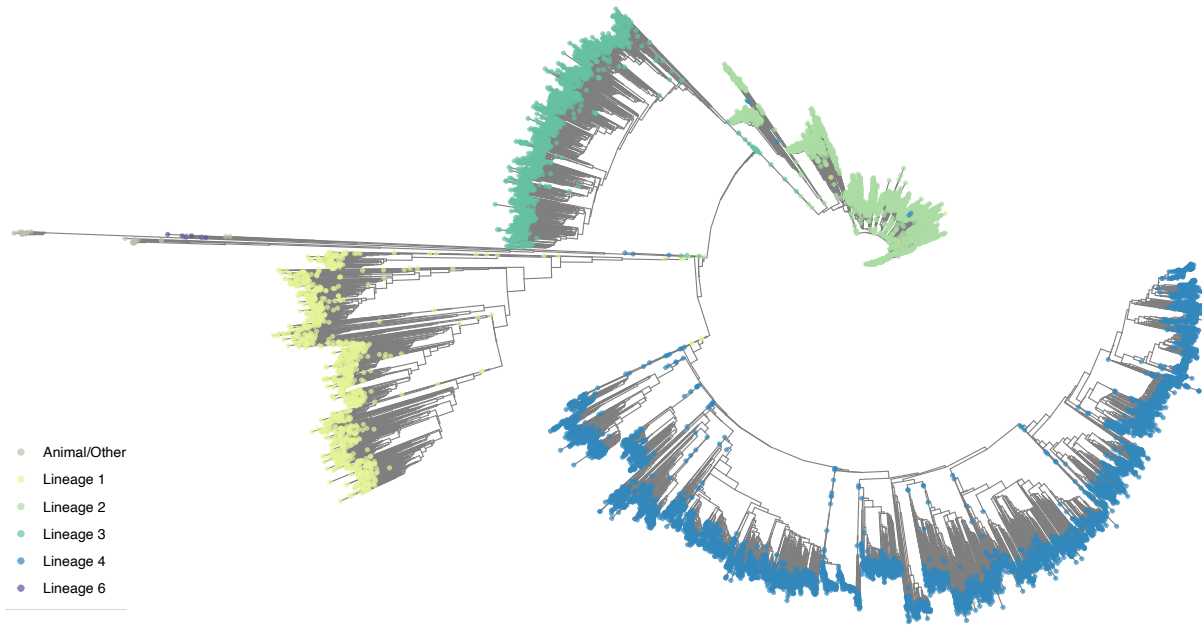


1104
1105 **Figure S3: A significant association between country and lineage can be seen**
1106 **in the CRyPTIC data.** Pearson's chi-squared test, $\chi^2 = 7935.2$, $df = 110$, $p < 2.2e-16$.
1107 The correlation plot indicates the relative contribution of each row-column pairing to the chi-
1108 square test score (%).

1109

1110

1111



1112

1113 **Figure S4: Phylogenetic tree of CRyPTIC *M. tuberculosis* clinical isolates.** A
1114 phylogenetic cladogram of 15,211 *M. tuberculosis* clinical isolates. A neighbour-joining tree was
1115 constructed from a pairwise distance matrix using *quicktree* (27). Coloured dots at the branch
1116 termini represent the lineage assigned to each isolate. “Animal/Other” includes 16 isolates that
1117 were assigned the following lineages: *M. caprae* (1), *M. bovis* (1), along with 17 isolates previously
1118 defined as representative for specific sub-lineages (58).
1119
1120
1121

1122

UNIQUEID	COUNTRY OF ORIGIN	LINEAGE
site.11.subj.XTB-18-224.lab.XTB-18-224.iso.1	UNKNOWN	Lineage 2
site.10.subj.YA00026182.lab.YA00026182.i so.1	ZAF	Lineage 4

1123 **Table S5: Sample information for isolates classified as resistant to all 13**
1124 **CRyPTIC drugs tested.** The country of origin is specified using the 3-letter country codes
1125 (alpha-3) defined by ISO 3166-1.
1126
1127

1128
1129

1130

	INH	RIF	EMB	LEV	MXF	AMI	KAN	BDQ	CFZ	DLM	LZD	ETH	RFB
INH	100.0	74.8	38.0	34.0	27.8	14.0	17.0	1.5	5.5	1.7	2.0	28.2	70.4
RIF	93.5	100.0	46.3	41.4	34.1	17.2	20.8	1.8	6.0	1.7	2.3	29.4	91.3
EMB	98.5	95.9	100.0	53.9	47.1	23.3	26.4	2.4	8.2	2.3	3.7	35.8	87.3
LEV	93.3	90.2	56.9	100.0	78.5	27.3	31.3	3.1	9.4	2.9	4.7	39.2	87.1
MXF	95.0	92.3	61.9	97.6	100.0	29.9	34.6	3.2	9.9	2.7	5.3	41.9	88.8
AMI	93.0	90.4	58.9	65.3	57.8	100.0	90.4	2.4	13.0	5.2	8.1	40.7	82.8
KAN	89.4	86.7	53.0	59.5	53.2	72.0	100.0	1.8	10.6	3.2	5.7	40.4	80.0
BDQ	79.4	77.8	49.5	60.7	49.5	20.0	18.9	100.0	52.4	12.9	14.0	34.9	76.9
CFZ	61.9	52.8	34.9	38.2	32.1	21.8	22.5	10.6	100.0	9.4	10.2	27.0	53.7
DLM	55.2	44.4	28.2	33.2	23.9	24.4	19.1	7.1	26.3	100.0	19.3	22.1	45.4
LZD	77.6	69.9	53.2	64.7	58.7	46.7	41.2	9.8	34.2	24.1	100.0	42.6	66.7
ETH	96.5	79.4	47.0	48.7	41.9	21.1	26.2	2.2	8.3	2.4	3.9	100.0	77.1
RFB	93.3	96.8	44.5	42.1	34.4	16.6	20.3	1.9	6.4	1.9	2.3	29.9	100.0

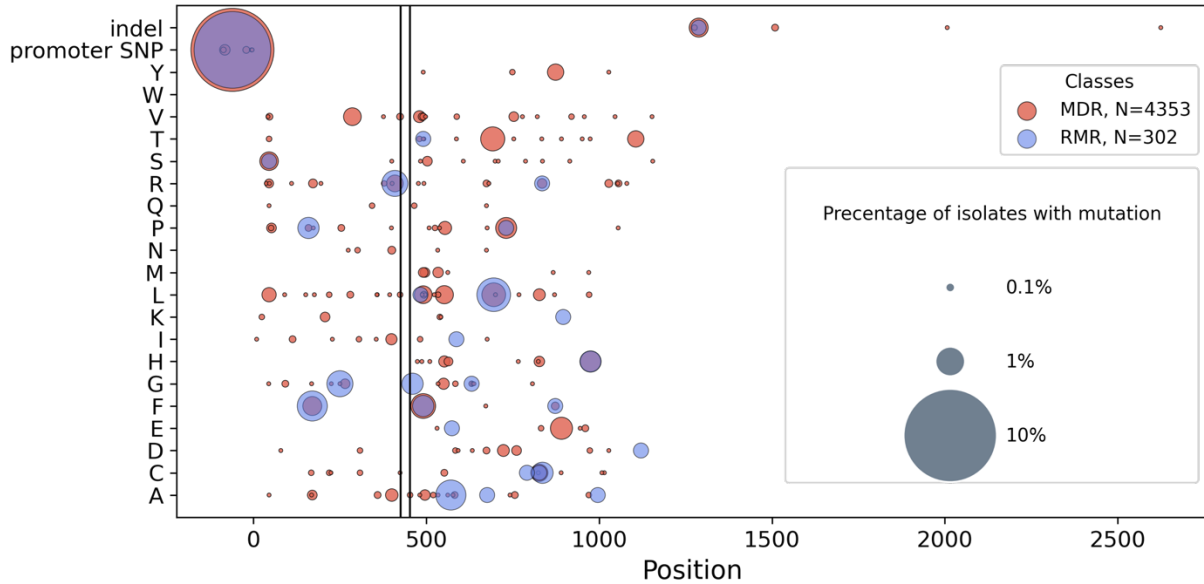
1131 **Table S6: Co-occurrence of antibiotic resistance in CRyPTIC *M. tuberculosis***

1132 **isolates.** The probability (%) of an isolate being resistant to Drug 2 (top) if it is resistant to Drug 1 (left). Drug acronyms: INH = isoniazid, RIF = rifampicin, EMB = ethambutol, LEV = levofloxacin, MXF = moxifloxacin, AMI = amikacin, KAN = kanamycin, BDQ = bedaquiline, CFZ = clofazimine, DLM = delamanid, LZD = linezolid, ETH = ethionamide, RFB = rifabutin.

1135

1136

1137



1138

1139 **Figure S6: Non-synonymous mutations found outside the RRDR of rpoB in RMR**
1140 **isolates and MDR isolates.** Presence of a coloured spot indicates that the mutation was
1141 found in RMR/MDR isolates and spot size corresponds to the proportion of RMR or MDR isolates
1142 carrying that mutation.

1143

1144

1145 **References**

1. WHO. Global Tuberculosis Report 2020. 2021;
2. Shinnick TM, Starks AM, Alexander HL, Castro KG. Evaluation of the Cepheid Xpert MTB/RIF assay. Expert review of molecular diagnostics. 2015 Jan;15(1):9–22.
3. Boehme CC, Nicol MP, Nabeta P, Michael JS, Gotuzzo E, Tahirli R, et al. Feasibility, diagnostic accuracy, and effectiveness of decentralised use of the Xpert MTB/RIF test for diagnosis of tuberculosis and multidrug resistance: a multicentre implementation study. Lancet (London, England). 2011 Apr 30;377(9776):1495–505.
4. Makhado NA, Matabane E, Faccin M, Pinçon C, Jouet A, Boutachkourt F, et al. Outbreak of multidrug-resistant tuberculosis in South Africa undetected by WHO-endorsed commercial tests: an observational study. The Lancet Infectious Diseases. 2018 Dec;18(12):1350–9.
5. Beckert P, Sanchez-Padilla E, Merker M, Dreyer V, Kohl TA, Utpatel C, et al. MDR *M. tuberculosis* outbreak clone in Eswatini missed by Xpert has elevated bedaquiline resistance dated to the pre-treatment era. Genome Medicine. 2020 Dec 25;12(1):104.
6. Sanchez-Padilla E, Merker M, Beckert P, Jochims F, Dlamini T, Kahn P, et al. Detection of Drug-Resistant Tuberculosis by Xpert MTB/RIF in Swaziland. New England Journal of Medicine. 2015 Mar 19;372(12):1181–2.
7. The CRyPTIC Consortium, 100 000 Genomes ProjecT. Prediction of Susceptibility to First-Line Tuberculosis Drugs by DNA Sequencing. New England Journal of Medicine. 2018 Oct 11;379(15):1403–15.
8. Pankhurst LJ, del Ojo Elias C, Votintseva AA, Walker TM, Cole K, Davies J, et al. Rapid, comprehensive, and affordable mycobacterial diagnosis with whole-genome sequencing: a prospective study. The Lancet Respiratory medicine. 2016 Jan;4(1):49–58.
9. Kalokhe AS, Shafiq M, Lee JC, Ray SM, Wang YF, Metchock B, et al. Multidrug-resistant tuberculosis drug susceptibility and molecular diagnostic testing. The American journal of the medical sciences. 2013 Feb;345(2):143–8.
10. Rancoita PM v, Cugnata F, Gibertoni Cruz AL, Borroni E, Hoosdally SJ, Walker TM, et al. Validating a 14-Drug Microtiter Plate Containing Bedaquiline and Delamanid for Large-Scale Research Susceptibility Testing of *Mycobacterium tuberculosis*. Antimicrobial agents and chemotherapy. 2018;62(9).
11. The CRyPTIC Consortium. Epidemiological cutoff values for a 96-well broth microdilution plate for high-throughput research antibiotic susceptibility testing of *M. tuberculosis*. European Respiratory Journal. 2022 Mar 17;2200239.
12. The CRyPTIC Consortium. Quantitative measurement of antibiotic resistance in *Mycobacterium tuberculosis* reveals genetic determinants of resistance and susceptibility in a target gene approach. bioRxiv. 2021;
13. The CRyPTIC Consortium. Predicting Susceptibility to First- and Second-line Tuberculosis Drugs by DNA sequencing and Machine Learning. In preparation.
14. The CRyPTIC Consortium. Genome-wide association studies of global *Mycobacterium tuberculosis* resistance to thirteen antimicrobials in 10,228 genomes. bioRxiv. 2021;
15. Sonnenkalb L, Carter J, Spitaleri A, Iqbal Z, Hunt M, Malone K, et al. Deciphering Bedaquiline and Clofazimine Resistance in Tuberculosis: An Evolutionary Medicine Approach. bioRxiv. 2021 Jan 1;2021.03.19.436148
16. Fowler PW, Gibertoni Cruz AL, Hoosdally SJ, Jarrett L, Borroni E, Chiacchiaretta M, et al. Automated detection of bacterial growth on 96-well plates for high-throughput drug susceptibility testing of *Mycobacterium tuberculosis*. Microbiology. 2018 Dec 1;164(12):1522–30.

1195 17. Fowler PW, Wright C, Spiers-Bowers H, Zhu T, Baeten EML, Hoosdally SW, et al.
1196 BashTheBug: a crowd of volunteers reproducibly and accurately measure the
1197 minimum inhibitory concentrations of 13 antitubercular drugs from photographs of 96-
1198 well broth microdilution plates. *bioRxiv*. 2021 Jan 1;2021.07.20.453060

1199 18. Hunt M, Letcher B, Malone KM, Nguyen G, Hall MB, Colquhoun RM, et al. Minos:
1200 variant adjudication and joint genotyping of cohorts of bacterial genomes. *bioRxiv*.
1201 2021 Jan 1;2021.09.15.460475.

1202 19. Li H, Durbin R. Fast and accurate short read alignment with Burrows-Wheeler
1203 transform. *Bioinformatics*. 2009 Jul 15;25(14):1754–60.

1204 20. Bolger AM, Lohse M, Usadel B. Trimmomatic: a flexible trimmer for Illumina
1205 sequence data. *Bioinformatics*. 2014 Aug 1;30(15):2114–20.

1206 21. Li H, Handsaker B, Wysoker A, Fennell T, Ruan J, Homer N, et al. The Sequence
1207 Alignment/Map format and SAMtools. *Bioinformatics* (Oxford, England). 2009 Aug
1208 15;25(16):2078–9.

1209 22. Iqbal Z, Caccamo M, Turner I, Flicek P, McVean G. De novo assembly and
1210 genotyping of variants using colored de Bruijn graphs. *Nature Genetics*. 2012 Feb
1211 8;44(2):226–32.

1212 23. Hunt M, Bradley P, Lapierre SG, Heys S, Thomsit M, Hall MB, et al. Antibiotic
1213 resistance prediction for *Mycobacterium tuberculosis* from genome sequence data with
1214 Mykrobe. *Wellcome open research*. 2019;4:191.

1215 24. Walker TM, Lalor MK, Broda A, Ortega LS, Morgan M, Parker L, et al. Assessment
1216 of *Mycobacterium tuberculosis* transmission in Oxfordshire, UK, 2007–12, with whole
1217 pathogen genome sequences: an observational study. *The Lancet Respiratory
1218 Medicine*. 2014 Apr;2(4):285–92.

1219 25. Miotto P, Tessema B, Tagliani E, Chindelevitch L, Starks AM, Emerson C, et al. A
1220 standardised method for interpreting the association between mutations and phenotypic
1221 drug resistance in *Mycobacterium tuberculosis*. *European Respiratory Journal*. 2017
1222 Dec;50(6):1701354.

1223 26. Walker TM, Miotto P, Köser CU, Fowler PW, Knaggs J, Iqbal Z, et al. The 2021
1224 WHO Catalogue of *Mycobacterium Tuberculosis* Complex Mutations Associated with
1225 Drug Resistance: A New Global Standard for Molecular Diagnostics. *SSRN Electronic
1226 Journal*. 2021;

1227 27. Howe K, Bateman A, Durbin R. QuickTree: building huge Neighbour-Joining trees of
1228 protein sequences. *Bioinformatics*. 2002 Nov 1;18(11):1546–7.

1229 28. Yu G. Using ggtree to Visualize Data on Tree-Like Structures. *Current Protocols in
1230 Bioinformatics*. 2020 Mar 5;69(1).

1231 29. Coscolla M, Gagneux S. Consequences of genomic diversity in *Mycobacterium
1232 tuberculosis*. *Seminars in Immunology*. 2014 Dec;26(6):431–44.

1233 30. Gagneux S. Ecology and evolution of *Mycobacterium tuberculosis*. *Nature Reviews
1234 Microbiology*. 2018 Apr 19;16(4):202–13.

1235 31. Freschi L, Vargas R, Husain A, Kamal SMM, Skrahina A, Tahseen S, et al. Population
1236 structure, biogeography and transmissibility of *Mycobacterium tuberculosis*. *Nature
1237 Communications*. 2021 Dec 20;12(1):6099.

1238 32. Ghimire S, Karki S, Maharjan B, Kosterink JGW, Touw DJ, van der Werf TS, et al.
1239 Treatment outcomes of patients with MDR-TB in Nepal on a current programmatic
1240 standardised regimen: retrospective single-centre study. *BMJ Open Respiratory
1241 Research*. 2020 Aug 12;7(1):e000606.

1242 33. Sharma R, Sharma SK, Singh BK, Mittal A, Kumar P. High degree of fluoroquinolone
1243 resistance among pulmonary tuberculosis patients in New Delhi, India. *The Indian
1244 journal of medical research*. 2019 Jan;149(1):62–6.

1245 34. Dijkstra JA, van der Laan T, Akkerman OW, Bolhuis MS, de Lange WCM, Kosterink
1246 JGW, et al. In Vitro Susceptibility of *Mycobacterium tuberculosis* to Amikacin,
1247 Kanamycin, and Capreomycin. *Antimicrobial Agents and Chemotherapy*. 2018
1248 Mar;62(3).

1249 35. Maitre T, Petitjean G, Chauffour A, Bernard C, el Helali N, Jarlier V, et al. Are
1250 moxifloxacin and levofloxacin equally effective to treat XDR tuberculosis? *Journal of*
1251 *Antimicrobial Chemotherapy*. 2017 Aug 1;72(8):2326–33.

1252 36. Berrada ZL, Lin S-YG, Rodwell TC, Nguyen D, Schechter GF, Pham L, et al. Rifabutin
1253 and rifampin resistance levels and associated rpoB mutations in clinical isolates of
1254 *Mycobacterium tuberculosis* complex. *Diagnostic Microbiology and Infectious*
1255 *Disease*. 2016 Jun;85(2):177–81.

1256 37. Ho J, Jelfs P, Sintchenko V. Fluoroquinolone resistance in non-multidrug-resistant
1257 tuberculosis—a surveillance study in New South Wales, Australia, and a review of
1258 global resistance rates. *International Journal of Infectious Diseases*. 2014 Sep;26:149–
1259 53.

1260 38. Singh R, Manjunatha U, Boshoff HIM, Ha YH, Niyomrattanakit P, Ledwidge R, et al.
1261 PA-824 Kills Nonreplicating *Mycobacterium tuberculosis* by Intracellular NO Release.
1262 *Science*. 2008 Nov 28;322(5906):1392–5.

1263 39. Hartkoorn RC, Uplekar S, Cole ST. Cross-Resistance between Clofazimine and
1264 Bedaquiline through Upregulation of MmpL5 in *Mycobacterium tuberculosis*.
1265 *Antimicrobial Agents and Chemotherapy*. 2014 May;58(5):2979–81.

1266 40. Degiacomi G, Sammartino JC, Sinigiani V, Marra P, Urbani A, Pasca MR. In vitro
1267 Study of Bedaquiline Resistance in *Mycobacterium tuberculosis* Multi-Drug Resistant
1268 Clinical Isolates. *Frontiers in microbiology*. 2020;11:559469.

1269 41. Almeida D, Ioerger T, Tyagi S, Li S-Y, Mdluli K, Andries K, et al. Mutations in pepQ
1270 Confer Low-Level Resistance to Bedaquiline and Clofazimine in *Mycobacterium*
1271 *tuberculosis*. *Antimicrobial Agents and Chemotherapy*. 2016 Aug;60(8):4590–9.

1272 42. Nimmo C, Millard J, van Dorp L, Brien K, Moodley S, Wolf A, et al. Population-level
1273 emergence of bedaquiline and clofazimine resistance-associated variants among
1274 patients with drug-resistant tuberculosis in southern Africa: a phenotypic and
1275 phylogenetic analysis. *The Lancet Microbe*. 2020 Aug;1(4):e165–74.

1276 43. Mvelase NR, Balakrishna Y, Lutchminarain K, Mlisana K. Evolving rifampicin and
1277 isoniazid mono-resistance in a high multidrug-resistant and extensively drug-resistant
1278 tuberculosis region: a retrospective data analysis. *BMJ Open*. 2019 Nov
1279 6;9(11):e031663.

1280 44. Villegas L, Otero L, Sterling TR, Huaman MA, van der Stuyft P, Gotuzzo E, et al.
1281 Prevalence, Risk Factors, and Treatment Outcomes of Isoniazid- and Rifampicin-
1282 Mono-Resistant Pulmonary Tuberculosis in Lima, Peru. *PLOS ONE*. 2016 Apr
1283 5;11(4):e0152933.

1284 45. Park S, Jo K-W, Lee S do, Kim WS, Shim TS. Treatment outcomes of rifampin-
1285 sparing treatment in patients with pulmonary tuberculosis with rifampin-mono-
1286 resistance or rifampin adverse events: A retrospective cohort analysis. *Respiratory*
1287 *Medicine*. 2017 Oct;131:43–8.

1288 46. Salaam-Dreyer Z, Streicher EM, Sirgel FA, Menardo F, Borrell S, Reinhard M, et al.
1289 Rifampicin-Monoresistant Tuberculosis Is Not the Same as Multidrug-Resistant
1290 Tuberculosis: a Descriptive Study from Khayelitsha, South Africa. *Antimicrobial*
1291 *Agents and Chemotherapy*. 2021 Oct 18;65(11).

1292 47. Pang Y, Lu J, Wang Y, Song Y, Wang S, Zhao Y. Study of the Rifampin
1293 Monoresistance Mechanism in *Mycobacterium tuberculosis*. *Antimicrobial Agents and*
1294 *Chemotherapy*. 2013 Feb;57(2):893–900.

1295 48. Kigozi E, Kasule GW, Musisi K, Lukoye D, Kyobe S, Katabazi FA, et al. Prevalence
1296 and patterns of rifampicin and isoniazid resistance conferring mutations in
1297 *Mycobacterium tuberculosis* isolates from Uganda. PLOS ONE. 2018 May
1298 30;13(5):e0198091.

1299 49. Dean AS, Zignol M, Cabibbe AM, Falzon D, Glaziou P, Cirillo DM, et al. Prevalence
1300 and genetic profiles of isoniazid resistance in tuberculosis patients: A multicountry
1301 analysis of cross-sectional data. PLOS Medicine. 2020 Jan 21;17(1):e1003008.

1302 50. Migliori GB, Langendam MW, D'Ambrosio L, Centis R, Blasi F, Huitric E, et al.
1303 Protecting the tuberculosis drug pipeline: stating the case for the rational use of
1304 fluoroquinolones. European Respiratory Journal. 2012 Oct;40(4):814–22.

1305 51. Heysell SK, Ahmed S, Rahman MdT, Akhanda MdW, Gleason AT, Ebers A, et al.
1306 Hearing loss with kanamycin treatment for multidrug-resistant tuberculosis in
1307 Bangladesh. European Respiratory Journal. 2018 Mar;51(3):1701778.

1308 52. WHO. Update on the use of nucleic acid amplification tests to detect TB and drug-
1309 resistant TB: rapid communication. 2021;

1310 53. Olaru ID, Heyckendorf J, Andres S, Kalsdorf B, Lange C. Bedaquiline-based treatment
1311 regimen for multidrug-resistant tuberculosis. European Respiratory Journal. 2017 May
1312 21;49(5):1700742.

1313 54. WHO. World Health Organization treatment guidelines for drug-resistant tuberculosis,
1314 2016 update. 2016;

1315 55. Huitric E, Verhasselt P, Koul A, Andries K, Hoffner S, Andersson DI. Rates and
1316 Mechanisms of Resistance Development in *Mycobacterium tuberculosis* to a Novel
1317 Diarylquinoline ATP Synthase Inhibitor. Antimicrobial Agents and Chemotherapy.
1318 2010 Mar;54(3):1022–8.

1319 56. Holt KE, McAdam P, Thai PVK, Thuong NTT, Ha DTM, Lan NN, et al. Frequent
1320 transmission of the *Mycobacterium tuberculosis* Beijing lineage and positive selection
1321 for the EsxW Beijing variant in Vietnam. Nature Genetics. 2018 Jun 21;50(6):849–56.

1322 57. Chiner-Oms Á, Comas I. Large genomics datasets shed light on the evolution of the
1323 *Mycobacterium tuberculosis* complex. Infection, Genetics and Evolution. 2019
1324 Aug;72:10–5.

1325 58. Borrell S, Trauner A, Brites D, Rigouts L, Loiseau C, Coscolla M, et al. Reference set
1326 of *Mycobacterium tuberculosis* clinical strains: A tool for research and product
1327 development. PLOS ONE. 2019 Mar 25;14(3):e0214088.

1328